Brazilian Journal of Geology

This is an open-access article distributed under the terms of the Creative Commons Attribution License (CC BY 4.0). Fonte: http://www.scielo.br/scielo.php?script=sci_arttext&pid=S2317-48892017000400561&lng=en&nrm=iso. Acesso em: 5 jan. 2018.

REFERÊNCIA

CAMPOS, Daniela Schievano de et al. Prospectivity analysis of gold and iron oxide copper-gold-(silver) mineralizations from the Faina Greenstone Belt, Brazil, using multiple data sets. **Brazilian Journal of Geology**, São Paulo, v. 47, n. 4, p. 561-590, out./dez. 2017. Disponível em: <http://www.scielo.br/scielo.php?script=sci_arttext&pid=S2317-48892017000400561&lng=en&nrm=iso>. Acesso em: 5 jan. 2018. doi: http://dx.doi.org/10.1590/2317-4889201720170012.

DOI: 10.1590/2317-4889201720170012

ARTICLE

Prospectivity analysis of gold and iron oxide copper-gold-(silver) mineralizations from the Faina Greenstone Belt, Brazil, using multiple data sets

Análises prospectivas em mineralizações hospedadas em depósitos orogênico e do tipo óxido de ferro-cobre-ouro-(prata) no Greenstone Belt Faina, Brasil, utilizando dados multifonte

Daniela Schievano de Campos[1]*, Adalene Moreira Silva[1], Catarina Laboure Bemfica Toledo[1], Marcelo Juliano de Carvalho[2], Vinícius Gomes Rodrigues[2], Kawinã Araujo[2]

ABSTRACT: The Faina Greenstone Belt is located in the southern sector of the Goiás Archean Block and has been investigated since the 18th century because of its gold deposits. Recent studies have revealed the polymetallic potential of the belt, which is indicated by anomalous levels of Ag, Cu, Fe and Co in addition to Mn, Ba, Li, Ni, Cr and Zn. This study was developed based on a detailed analysis of two selected target sites, Cascavel and Tinteiro, and multiple data sets, such as airborne geophysics, geochemistry and geological information. These datasets were used to create a final prospectivity map using the fuzzy logic technique. The gold mineralization of Cascavel target is inserted in an orogenic system and occurs in two overlapping quartz veins systems, called Mestre-Cascavel and Cuca, embedded in quartzite with an average thickness 50 cm and guidance N45º–60ºW/25ºSW with free coarse gold in grains 2–3 mm to 3 cm. The prospectivity map created for this prospect generated four first-order favorable areas for mineralization and new medium-favorability foci. The Tinteiro area, derived from studies conducted by Orinoco do Brasil Mineração Ltda., shows polymetallic mineralization associated with an iron oxide-copper-gold ore deposit (IOCG) system posterior to Cascavel target mineralization. Its prospectivity map generated 19 new target sites with the potential for Au, Cu and Ag mineralization, suggesting new directions for future prospecting programs.

KEYWORDS: Faina Greenstone Belt; aeromagnetometry; gamma spectrometry; gold mineralization; polymetallic mineralization; fuzzy logic.

RESUMO: *O Greenstone Belt Faina está localizado na porção sul do Bloco Arqueano de Goiás e vem sendo pesquisado desde o século XVIII por conta dos seus depósitos auríferos. Estudos recentes revelaram o potencial polimetálico do cinturão, em razão dos valores anômalos de Ag, Cu, Fe e Co, além de Mn, Ba, Li, Ni, Cr e Zn. Este estudo foi desenvolvido por meio da caracterização de dois alvos selecionados, Cascavel e Tinteiro, utilizando dados multifonte, tais como aerogeofísica de alta resolução, geoquímica e geologia. Esses dados foram integrados para criar um mapa prospectivo final utilizando a técnica lógica fuzzy. A mineralização aurífera do alvo Cascavel está inserida em um sistema orogênico e ocorre em dois sistemas de veios de quartzo superpostos, denominados de Mestre-Cascavel e Cuca, encaixados em quartzitos e com espessura média de 50 cm e orientação N45º–60ºW/25ºSW com a presença de ouro livre em grãos de 2–3 mm até 3 cm. O mapa prospectivo criado para esse prospecto indicou quatro áreas mineralizadas com favorabilidade de primeira ordem e novos focos com média favorabilidade. O alvo Tinteiro, derivado de estudos realizados pela empresa Orinoco do Brasil Mineração Ltda., mostra uma mineralização polimetálica associada a depósito do tipo óxido de ferro-obre-ouro-(prata), posterior à mineralização do alvo Cascavel. Seu mapa prospectivo apontou 19 novos focos com alta potencialidade para mineralização de Au, Cu e Ag, sugerindo novas direções para futuros programas prospectivos.*

PALAVRAS-CHAVES: *Greenstone Belt Faina; aeromagnetometria; gamaespectometria; mineralização aurífera; mineralização polimetálica; lógica fuzzy.*

[1]Institute of Geosciences, Universidade de Brasília – UnB, Brasília (DF), Brazil. *E-mails: dani.schievano@gmail.com, adalene.silva@gmail.com, catarina.laboure.toledo@gmail.com*

[2]Orinoco do Brasil Mineração Ltda., Goiás (GO), Brazil. *E-mails: marcelo@orinocogold.com, vinicius@orinocogold.com, kawina@orinocogold.com*

*Corresponding author.

Manuscript ID: 20170012. **Received in:** 01/26/2017. **Approved in:** 08/29/2017.

INTRODUCTION

Globally, mining companies seek to utilize prospective efficient methods that decrease costs during mineral exploration stages. To achieve such goals, they must use techniques that efficiently aggregate the data generated in the different stages of a given study by focusing on models that have a greater likelihood of estimating deposits (Robert *et al.* 2007). Magnetic surveys coupled with high-resolution gamma spectrometry data represent available technology in airborne geophysics for the detection of relevant structures for mineral exploration, and they have been shown to be efficient in the selection of follow-up target sites in tropical terranes (Silva *et al.* 2012, Carrino *et al.* 2011).

The Faina Greenstone Belt is the target of this study, and, along with the Pilar de Goiás, Guarinos, Crixás and Serra de Santa Rita belts, it is part of the granite-greenstone terranes of the Archean-Paleoproterozoic terrane of Goiás, which is located in the northern sector of the Brasília Belt (Pimentel *et al.* 2004, Jost *et al*. 2005, Jost *et al*. 2013). This region has been investigated since the time of the *Bandeirantes* explorers (18th and 19th centuries) and shows the potential to host gold (Au) mineralizations. Several companies have mined in the area, including the well-known Metais de Goiás S.A. (METAGO), Western Mining Co., Amazônia Mineração and Troy Resources Brazil.

The discovery of Sertão, a low-tonnage and high-grade gold mine, had a positive impact on the local economy and on the cities of Faina and Goiás. The mine was explored in the period from 2000 to 2007 by Sertão Mineração Ltda., which ceased its activities after exploiting the oxidized ore to a depth of 40 m. The company reported the extraction more than 250,000 ounces of gold, at an average recovered grade of 24.95 g/t Au. Since 2011, the area has been studied by Yamana Gold Inc. and Orinoco do Brasil Mineração Ltda.

Orinoco do Brasil Mineração Ltda. is particularly relevant because of its investments in the Faina Greenstone Belt, including an innovative exploration program for known target sites, such as Cascavel, and the discovery of the new target sites of Tinteiro and Eliseu. The new target sites indicate a potential for gold and polymetallic mineralizations in the region. Additionally, the company resumed and intensified their studies in the Mina de Sertão site, and they plan to reopen it as an underground mine (http://orinocogold.com/).

This study focuses on detailing two selected target mineralization sites (Cascavel and Tinteiro) of the Faina Greenstone Belt using a methodology based on the processing and interpretation of aeromagnetic, gamma spectrometry and geochemical data. The data were then integrated into mineral favorability models using fuzzy logic, and the methodological steps were derived from the exploration program proposed by Pan and Harris (2000), Harris and Sanborn-Barrie (2006) and modified from Nykänen (2008) and Silva *et al.* (2012) (Fig. 1).

GEOLOGIC CONTEXT AND MINERALIZATION IN THE FAINA GREENSTONE BELT

Regional Geology

The study area is located within the Archean-Paleoproterozoic Terrane of Goiás in the Brasília fold belt within Tocantins Province (Pimentel *et al.* 2000, Queiroz *et al.* 2008, Jost *et al.* 2013) (Fig. 2). The Archean-Paleoproterozoic Terrane of Goiás extends over approximately 50,000 km^2, and 30% of it consists of volcano-sedimentary sequences of the greenstone belt type and 70% comprises granite-gneiss rocks, thus forming a typical granite-greenstone terrane (Fig. 2) (Almeida *et al.* 1977, Danni *et al.* 1981, Jost & Oliveira 1991, Kuyumjian & Jost 2006). The greenstone belts occur in five narrow belts, three of which (Crixás, Guarinos and Pilar de Goiás) are located in the northern end, and two of them (Serra de Santa Rita and Faina) are located in the southern end. These belts host important gold deposits and are preserved in elongated synforms isolated by the Archean granite-gneiss complexes Hidrolina, Moquém, Caiamar, Anta, Caiçara and Uvá (Pimentel *et al.* 2000, Jost & Fortes 2001) (Fig. 2).

The greenstone belts Serra de Santa Rita and Faina are located in the southern part of the granite-greenstone terrane, and they are structured in a syncline that is NW-SE aligned, 150-km long and 6 km wide (Kuyumjian & Jost 2006, Baêta *et al.* 1998). These belts are separated by the strike-slip Faina Fault, which strikes to N30E (Resende *et al.* 1998), and they are located between two granite-gneiss complexes with distinct geologic evolution. The Caiçara Complex to the north consists of 3.1 Ga old tonalitic gneisses and intrusive granodiorites, monzogranites and charnockite series, with ages between 2838 and 2818 Ma (Beghelli Jr. 2012). The Uvá Complex to the south consists of tonalitic gneisses and polydeformed granodiorites and dioritic rocks with crystallization ages from 3040 to 2930 Ma and granitic tabular bodies dating between 2876 and 2846 Ma (Jost *et al.* 2013). The contacts between the granite-gneiss complexes and supracrustal rocks are intrusive or tectonic and marked by inverse shear zones with high angles converging to the northeast that completely obliterate the original architecture of these belts (Resende *et al.* 1998, Jost *et al.* 2005).

Faina and Serra de Santa Rita Greenstone Belts

The lower stratigraphic sections of the Faina and Serra de Santa Rita greenstone belts are similar, and from the base to the top, they include metakomatiites (Manoel Leocádio Formation) and metabasalts (Digo-Digo Formation). In the Serra de Santa Rita Belt, the Digo-Digo Formation consists of metabasalts and felsic metapyroclastic rocks, which are absent in the Faina Greenstone Belt. This basal unit is overlapped in both belts by distinct metasedimentary sequences,

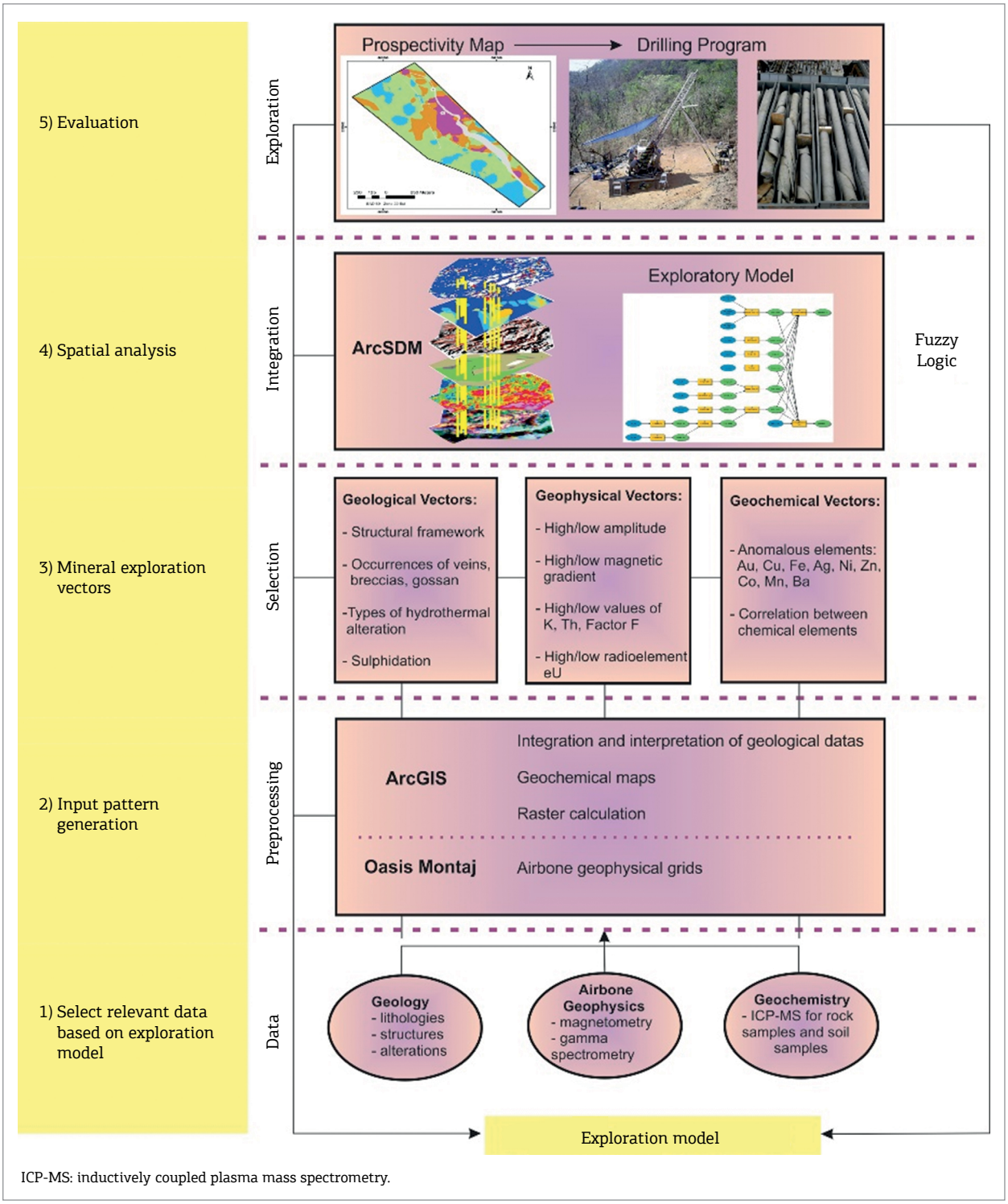

ICP-MS: inductively coupled plasma mass spectrometry.

Figure 1. The main steps of the mineral exploration model. This diagram is based in the method suggested by Pan and Harris (2000) and Harris and Sanborn-Barrie (2006) and adapted from Nykänen (2008) and Silva *et al.* (2012).

indicating different paleogeographic environments and depositional regimes in the basin (Resente *et al.* 1998) (Fig. 3).

In the Faina Greenstone Belt, the metasedimentary unit is represented by the Furna Rica Group, which is formed from the base to the top by records of two transgressive shelf sedimentary cycles (Resende *et al.* 1998). The first cycle begins with metaconglomerate lenses along with orthoquartzites, metapelites, carbonaceous schists and banded iron-formations (BIFs) from the Fazenda Tanque Formation laying on an angular unconformity over the underlying metavolcanic unit. The second cycle is represented by metaconglomerates, orthoquartzites and metapelites of the Serra de São José Formation covered by marbles and the iron formations of the Serra do Tatu Formation. The two sedimentary cycles are separated by an erosional unconformity indicated in Figure 3 as the metasedimentary Units A and B (Toledo *et al.* 2014).

The metasedimentary record of the Serra de Santa Rita Greenstone Belt is represented by the Fazenda Paraíso Group, which was formed at the base by carbon schists, metachert, iron formations, calc-schists and marbles. The top of the sequence is covered by metagreywackes from the Fazenda Cruzeiro Formation, and its sedimentation occurred in a deep marine environment and progressed to a shallower environment. In the Faina belt, shelf sedimentation occurred in two transgressive cycles of increasing depth (Resende *et al.* 1998). Geochemical data from the detrital rocks along the stratigraphic sections show that the Sm/Nd (T_{DM}) model ages of the source area decreased from 3.1 to 2.8 Ga. Additionally, the sediments originated from mafic/ultramafic sources in the initial stages of deposition, with an increase of felsic components towards the top of the sequence (Resende *et al.* 1999).

Mineralization

In the study area, the Sertão Mine and Cascavel prospect stand out because they both have significant potential for continuous resource exploration and definition projects. The Sertão Mine and the Cascavel prospect occur in the same structural context. The gold mineralization is of the *lode* type, and quartz veins are structurally controlled by

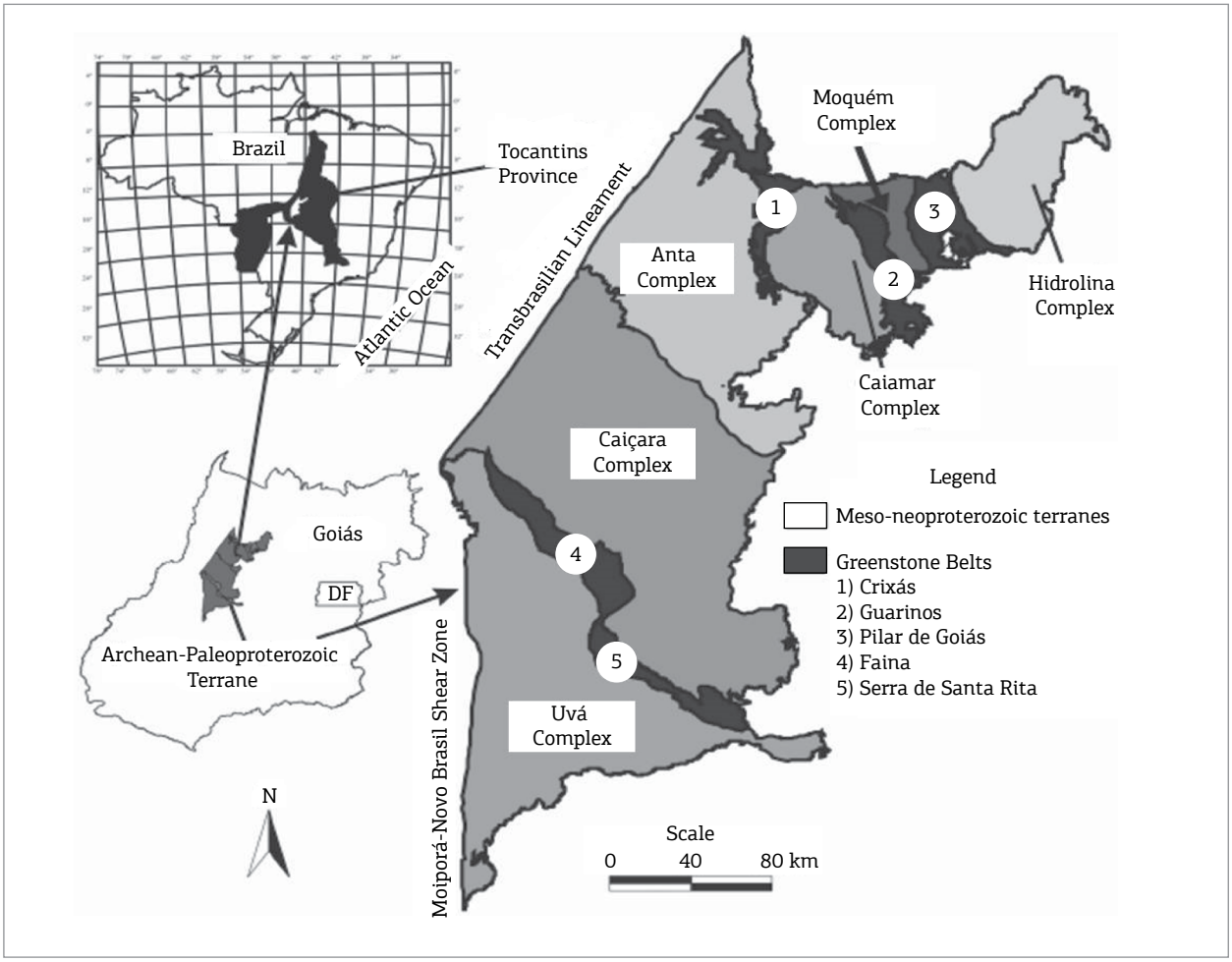

Figure 2. Simplified geologic map of the Archean-Paleoproterozoic Terrane in Goiás (Pimentel *et al.* 2000).

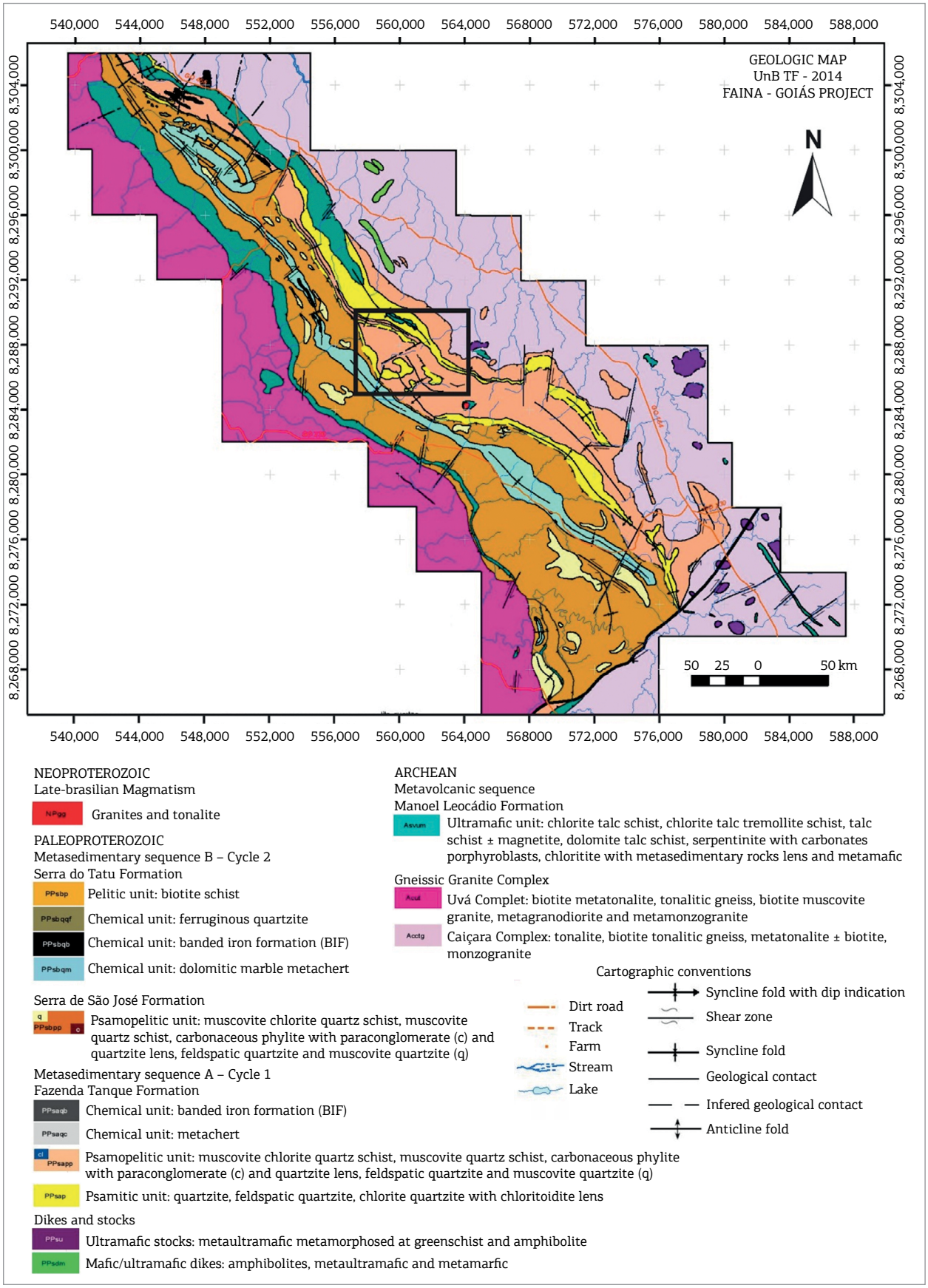

Figure 3. Simplified regional geologic map of the Faina Greenstone Belt produced by Toledo *et al.* (2014). The black polygon indicates the study area mapped at the 1:10,000 scale.

thrust faults and embedded in chlorite-quartz-schists of the second sedimentary cycle (Sertão) and feldspathic quartzites of the first sedimentary cycle (Cascavel). According to the data provided by Orinoco do Brasil Mineração Ltda., mineralized quartz veins extend along the direction and dip of the shear zone and appear to occur in structures of the second and third order as well. The locations of the Sertão mine and other study sites are indicated in Figure 4.

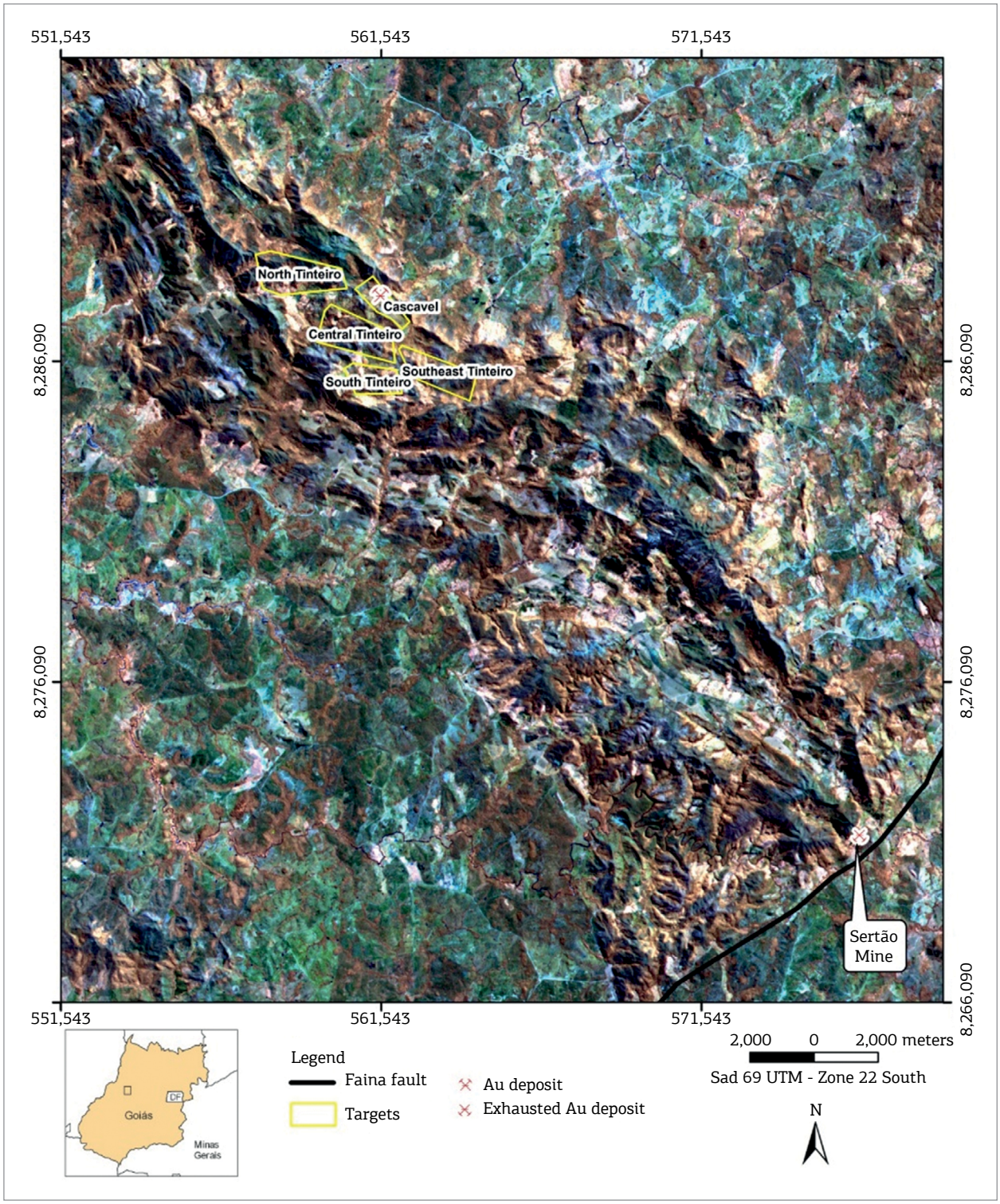

Figure 4. ETM+/Landsat 7 band 4, 5, 3 (RGB) color composite, partially covering the Faina Greenstone Belt. Sertão Mine and Cascavel, North, Central, South and Southeast Tinteiro prospects are indicated by yellow polygons.

The gold mineralizations inserted in the Cascavel prospect are characterized by the presence of coarse free gold with grain sizes varying from 2–3 mm to 3 cm (Jost *et al.* 2014), and they are found in association with quartz veins with thicknesses of 1 cm and a pinkish coloration arranged in continuity with the tectonic foliation of the host rocks. The quartz veins are associated with shear zones that intercept the feldspathic quartzites occurring at the base of the first sedimentary cycle (metasedimentary sequence A). Lenses and dolomite layers hosting mineralizations rich in Cu, Ag and W also occur at this site.

The Tinteiro prospect is subdivided into subareas south, central, north and southeast Tinteiro (Fig. 4). It represents a recent discovery by Orinoco do Brasil Mineração Ltda., is located in the metasedimentary sequence of the first depositional cycle, and it alternates with quartzites, metapelites and metacherts. The analysis of the rock outcrops, hand samples and core samples suggests a different context from that of the previous sites. Hydrothermal alteration is represented by sericitic halos with chloritoid, and hematite breccias associated with metacherts. The main control of the hydrothermal alteration comprises faults in NE, NW and E-W directions that intersect the rocks in the Faina Greenstone Belt. The hydrothermal alteration zones are related to the polymetallic mineralization of gold and copper in high concentrations as well as that of cobalt, barium, silver, uranium and iron. According to studies undertaken by Orinoco do Brasil Mineração Ltda., the accumulation of these metals occurred after the orogenic gold mineralization in an iron oxide copper gold ore deposit (IOCG) system.

MULTIPLE DATA SETS

The Faina Greenstone Belt was covered by aeromagnetic and high-resolution gamma spectrometry surveys covering a total area of 1,562.38 km^2 and with a flight altitude 50 m above the terrain and flight lines spaced 200 m apart in a N-S direction and control lines spaced 1,000 m apart in an E-W direction. A detailed area was covered by flight and control lines spaced 100 and 500 m apart, respectively, over the Cascavel and Tinteiro sites. The aeromagnetic and gamma spectrometry data grids were created using the software Oasis Montaj (Geosoft Inc.). The gamma spectrometry data were interpolated using a bi-directional method with the grid cell size set to 25% of the distance between flight lines.

Images from the Landsat 7 Enhanced Thematic Mapper Plus (ETM+) sensor was used to interpret the main geological features using the bands 4, 5, 7 RGB color composite, fused with the band 8 through a principal component algorithm. The image from path/row 223/071 was made available by Orinoco do Brasil Mineração Ltda.

In this study, a geologic map that covers the Faina Greenstone Belt and part of the Serra de Santa Rita Greenstone Belt at a 1:25,000 scale was used (Toledo *et al.* 2014) along with geologic data obtained from two field trips. The geologic mapping was performed at a 1:10,000 scale for the Cascavel and Tinteiro target sites. For the final integration of the results, geologic data provided by Orinoco do Brasil Mineração Ltda. were integrated. The geologic maps were created using ArcMap software (version 9.3) (ESRI).

To characterize the mineralogical and chemical behavior of the mineralized zones of the region, 7 of the 50 bore holes that intercepted the mineralized bodies of the Cascavel and Tinteiro target sites, which were made available by Orinoco do Brasil Mineração Ltda., were selected.

Petrographic studies of the transmitted and reflected light were undertaken using 70 thin polished sections and an Olympus BX60FS microscope (Olympus Optical Co. Ltd.), which was made available by the Laboratory of Microscopy of the University of Brasília (UnB). These analyses aimed to identify and characterize the hydrothermal alterations and mineralization zones.

Chemical mineral analyses were conducted in the Electronic Microprobe Laboratory of the Institute of Geosciences (UnB) using the superprobe model JEOL JXA-8230. The voltages used were 15 and 20 kV. Specific minerals were analyzed when required to assist in the petrographic descriptions and in the mineralogical characterizations of the hydrothermal alteration zones.

Geochemical data comprise major, minor and trace elements of the mineralized zones and its surroundings. These data were collected in samples obtained from boreholes, rocks and soil provided by the companies Troy Exploração Mineral Ltda. and Orinoco do Brasil Mineração Ltda. The analyses included a screen fire assay and inductively coupled plasma mass spectrometry (ICP-MS), which were conducted by the laboratories ALS Minerals, Intertek, SGS Minerals Services and ACME Analytical Laboratories Ltd. The chemical elements included in this study were those that exhibited anomalous concentrations in certain boreholes and field samples and included Au, Cu, Ag, Ni, Fe, Co and Ba, as well as certain pathfinder elements. The anomalous elements were selected for identifying anomalous zones and determine the correlation between these elements and the previously mapped geological-structural features.

The integration of all data was conducted using ArcSDM software (version 9.3) (ESRI), with the objective of creating the final exploration map using fuzzy logic tecnhique.

DATA PROCESSING AND INTERPRETATION

Geophysical Data

The high-resolution airborne geophysical data partially covering the Faina Greenstone Belt were processed following pre-processing and processing methods (interpolation and microleveling). After the grid interpolation of the anomalous magnetic field, the K (%), eTh (ppm), eU (ppm) channels, other products were generated and transformed from the data obtained at the 200 m intervals. Similarly, data obtained at the 100 m intervals were used to map hydrothermal halos and structures related to the Cascavel and north, south, central and southeast Tinteiro target sites (Fig. 4).

Aeromagnetic Data

These data were processed using efficient techniques to determine the geometric parameters and identify the geological and structural limits, geologic feature depths and structural measurements, such as the amplitude and inclination of the analytic signal, vertical and horizontal derivatives (X and Y), and amplitude of the total horizontal gradient. These products were used to map shear zones known to host gold and polymetallic mineralizations as well as their extensions in the sub-surface and across flattened areas that may have the potential to host Au or Cu-Au-(Ag). Figures 5A-5E illustrates the processes involved in the production of the following products for the Faina Greenstone Belt and the target sites: total magnetic intensity reduced from International Geomagnetic Reference Field (IGRF) (TMI), vertical derivative (Dz), horizontal derivative in X (Dx), horizontal derivative in Y (Dy) and analytic signal amplitude (ASA).

Gamma Spectrometry Data

The gamma ray aerial survey shows the geochemical variations of potassium, uranium and thorium up to a depth of 30 cm from the Earth's surface, and the main variations of these three radioelements translate into signatures that can be used to identify each type of rock (Dickson & Scott 1997). This geophysical method is a useful tool for geological mapping, and identification of hydrothermal alteration areas in different geological environments.

The processing of gamma spectrometry data was used to produce images of the K (%), eU (ppm) and eTh (ppm) channels, and a composite ternary RGB radiometric image (Figs. 6A-6D).

Additionally, image of the Fk factor, known as parameter F, was obtained, and it indicates the enrichment of potassium relative to thorium as well as hydrothermal alteration zones associated with mineralization (Gnojek & Prichystal 1985). Fk is calculated as follows: Fk = K*eU/eTh.

Interpretation of Aeromagnetic Data

The analysis of the anomalous magnetic field was performed using linear transformations, such as the horizontal derivatives in x and y (Dx, Dy) and the vertical derivative (Dz), to generate the image of the analytic signal amplitude (ASA) (Roest *et al*. 1992). The ASA was used to identify a number of the main magnetic bodies in the area and was of great importance to this study because certain hydrothermal alterations in the Tinteiro site and along the greenstone are associated with magnetite, which was confirmed in the geologic mapping. These results indicate that magnetic bodies are identified as quartzite and metachert layers with hydrothermal alterations that consist of massive iron oxide.

The identification and characterization of the magnetic structures were obtained by interpreting the vertical derivative Dz (Fig. 5E) (Evjen 1936) and complemented with the analysis of the horizontal derivatives in X and Y. It is noteworthy that the lineament term used here represents a straight or curved surface feature capable of being mapped, and it may be related to faults, fractures of other structures (Sabins 1996). This concept was extrapolated to the analysis of magnetic data, in which the lineaments are preferably mapped as magnetic highs. The identification of structures in magnetic valleys was incorporated in the interpretation to complement the structural framework. The methodology to identify the structural lineaments and the known structural groups are described next.

From the vertical derivative (Dz), the main lineaments mapped in the Faina Greenstone Belt were identified using the horizontal derivatives in x and y and the RGB (453) image of the Landsat 7 ETM+ sensor. Thus, the structural measurements obtained in the field confirmed that the main lineaments are aligned NW-SE, NE-SW and E-W (Fig. 7).

Interpretation of Gamma Spectrometry Data

The mineralizations hosted in the Faina Belt are associated with hydrothermal processes, such as potassification, sericitization, chloritization, silicification, carbonatation and sulphitation. The occurrence of minerals generated by potassic alterations, such as sericite, biotite and potassium feldspar, warrants the use of gamma spectrometry as a key tool in this study.

The domains represented by low levels of the three radioelements are represented in the ternary map in dark colors (black to dark blue) and indicate mafic-ultramafic rocks at the base of the stratigraphic sequence (Fig. 6D). These lithotypes are found in the W-SW and NE portions of the area.

Within the metasedimentary sequence, a domain with low levels of K (%), eTh and eU is observed, and it was formed by dolomites and quartzites rich in massive iron oxide.

Certain domains identified in the map were easily correlated with the lithology observed in the field. However, in certain areas, this correlation was not effective and required additional attention and caution in the data interpretation.

Geologic Data

Geologic mapping at the scale 1:10,000 (Fig. 8) was conducted for the Cascavel and Tinteiro target sites. The data show that they are hosted in rocks belonging to the first depositional cycle proposed by Resende *et al.* (1998). The geologic units in these areas are ultramafic schists of the volcanic sequence and rocks of the metasedimentary sequence A

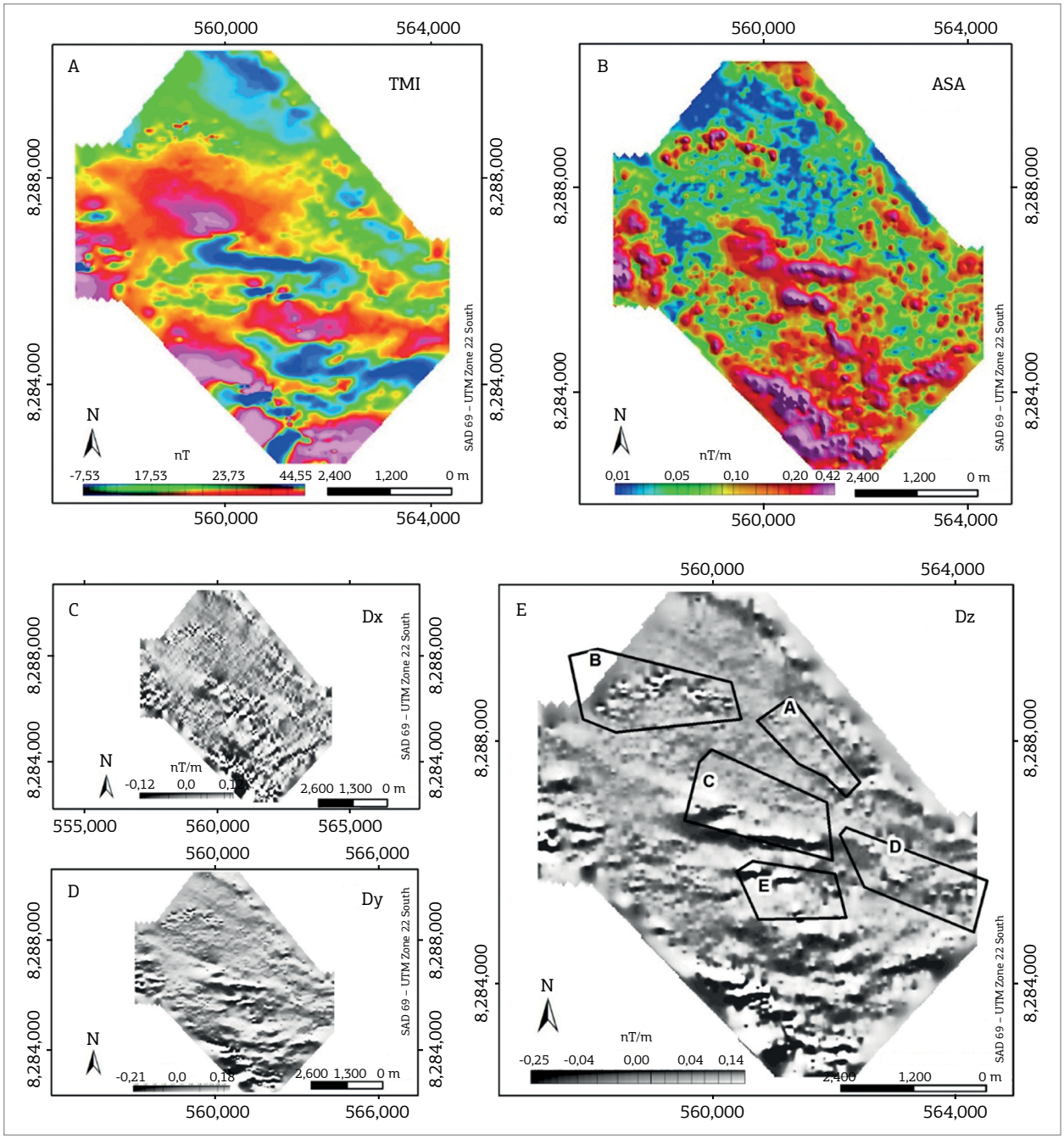

Figure 5. Main aeromagnetic products: (A) TMI; (B) ASA; (C) Dx; (D) Dy; and (E) Dz. The black outline indicates the main sites analyzed in this study: A – Cascavel, B – North Tinteiro, C – Central Tinteiro, D – Southeast Tinteiro and E – South Tinteiro.

(Toledo *et al.* 2014). The volcanic sequence is characterized by a small talc-schist lens within a package of metacherts in the southeastern sector of the North Tinteiro site. The metasedimentary sequence A is represented in the area by quartzites, feldspathic quartzites, metapelites, metarhythmites, metacherts, dolomitic marbles and carbonaceous schists.

Geochemical Data

The geochemical data obtained from the rock samples were used to create geochemical maps for each element that indicated their distribution at the site and their correlation with other elements. Some associations between elements were corroborated during the geochemical analysis of the borehole cores.

Soil samples were analyzed only for gold; therefore, it was difficult to use these data to create element maps. However, the geochemistry of the soil was useful in the validation of zones with high mineral favorability obtained according to the different prospecting scenarios.

POLYMETALLIC AND GOLD MINERALIZATIONS IN THE FAINA GREENSTONE BELT

Cascavel Target

Lithological and Structural Controls

The Cascavel prospect is located on the east border of the Faina Belt, where rocks belonging to the first depositional cycle are exposed. The main lithotypes found at this site belong to the metasedimentary Sequence A (Fig. 3) and consist of quartzites, metapelites, dolomitic marble and metarhythmites with carbonaceous schist lenses (Figs. 9A-9D). The mineralized zone is associated with the quartzite package, which can be subdivided into three types: pure quartzite or quartzite with muscovite, feldspathic quartzite and quartzite with green muscovite. The mineralization is hosted on the feldspathic quartzite.

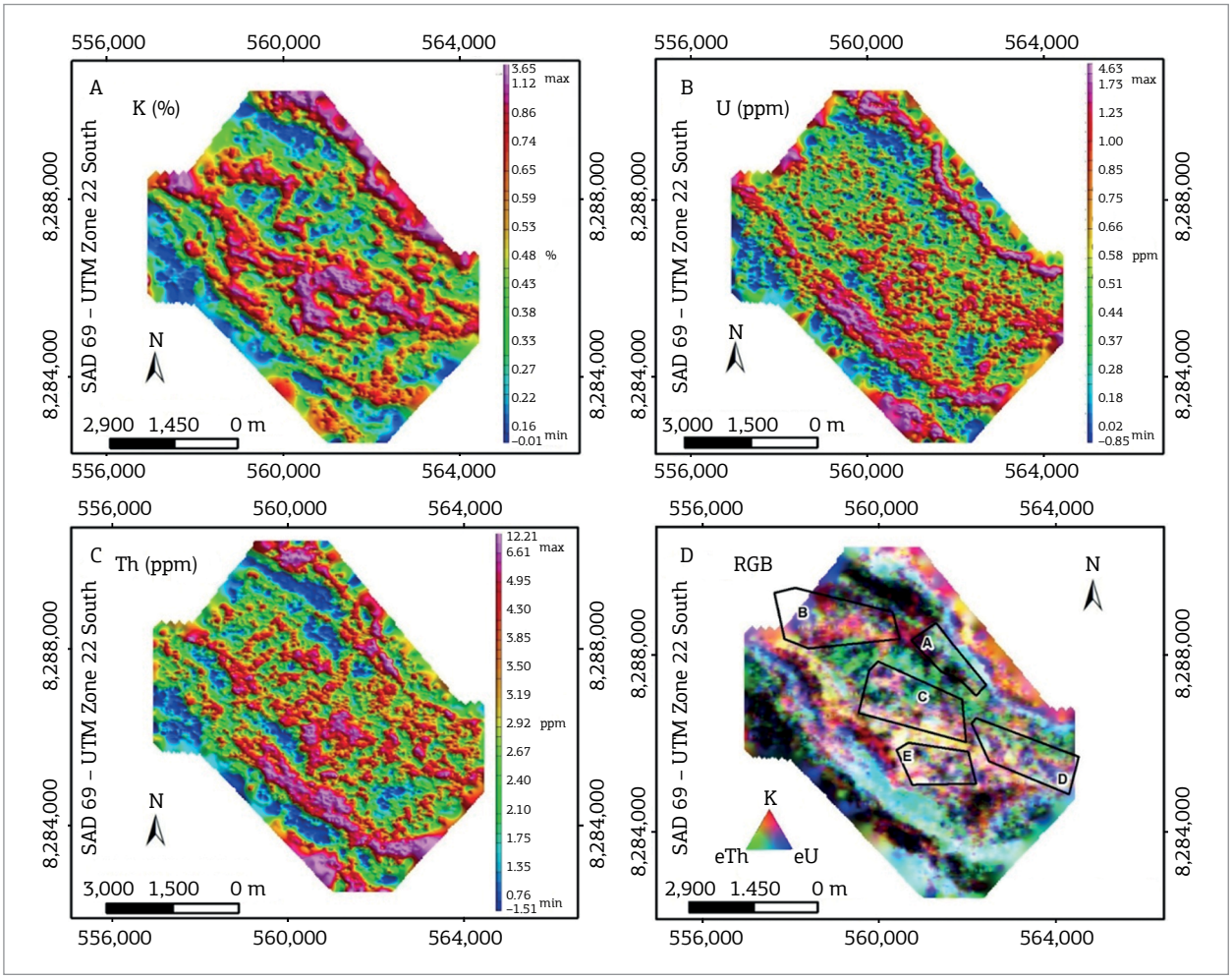

Figure 6. (A) K (%); (B) eU (ppm); (C) eTh (ppm) concentrations used to identify the hydrothermal alteration zones; and (D) RGB image, which is essential for the geologic mapping and the black outlines indicate the target sites (A – Cascavel, B – North Tinteiro, C – Central Tinteiro, D – Southeast Tinteiro and E – South Tinteiro).

The pure quartzite (Fig. 9A) is yellowish to pink, fine-grained and highly foliated, sometimes weathered, and it presents a granoblastic texture of and a modal composition of quartz (60–80%) and muscovite (20–30%) as the major minerals. Tourmaline and magnetite (locally) appear as accessory minerals. This rock may show crystals or carbonate pockets consistent with the main foliation, and the quartz is generally recrystallized.

The feldspathic quartzite (Fig. 9B) shows a similar composition to the package previously described (carbonate and muscovite), although it is characterized by the presence of potassium feldspar clasts. In the geologic map, it was identified as a thin lens outcropping in the central section of the syncline. In the borehole cores, this lithotype appears at the base of nearly all quartzite packages and shows transitional contact with pure quartzite.

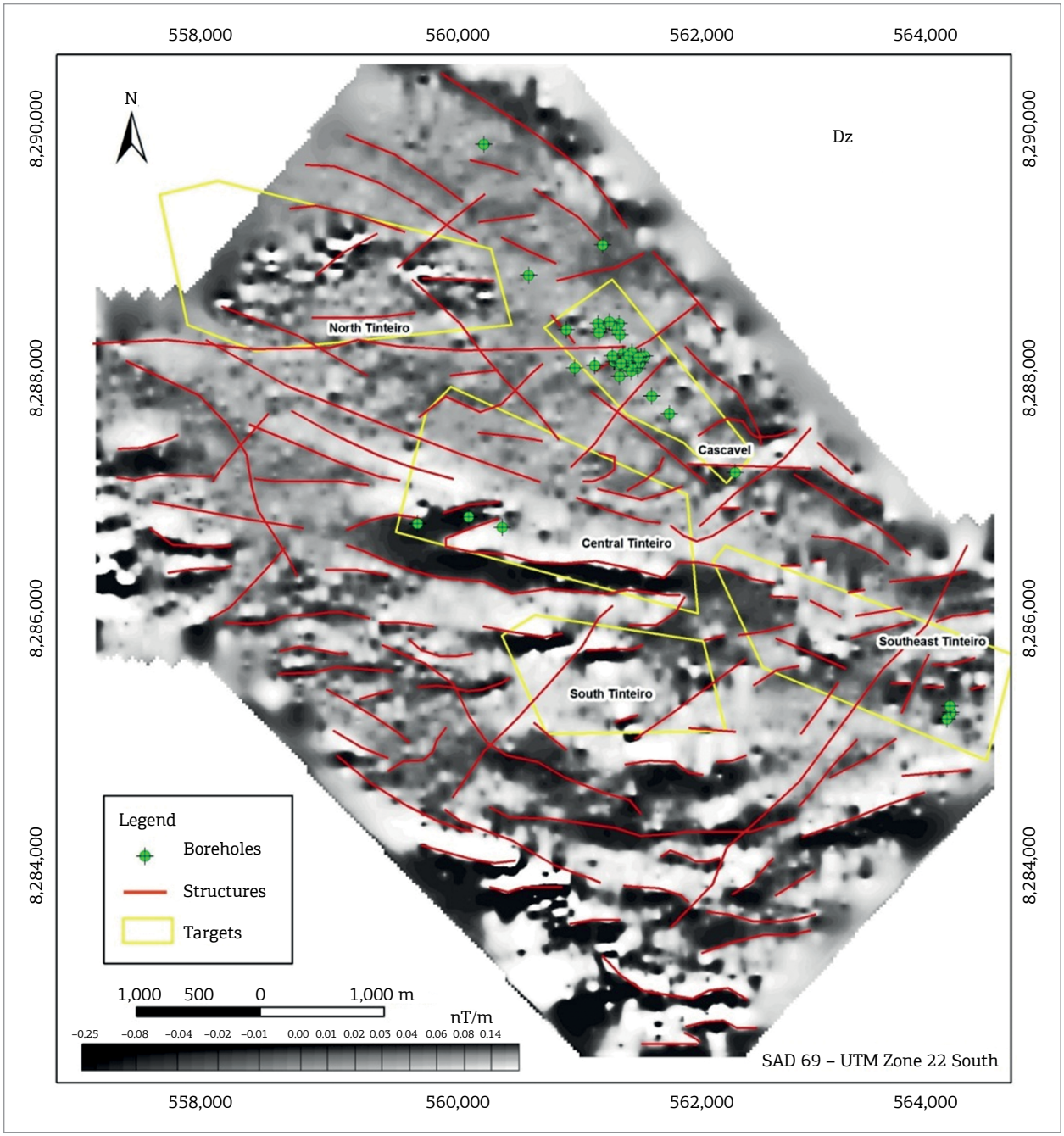

Figure 7. Map showing the first vertical derivative (Dz) of the TMI in the study area and identifying the main geologic structures interpreted based on the Dz, Dy, and RGB 453 image of the Landsat 7 ETM+ sensor. The boreholes conducted by the Orinoco do Brasil Mineração Ltda. are indicated by the green marker.

The quartzite with green muscovite is generally found associated with shear zones and it is considered a hydrothermal halo external to the mineralization. In this site, the gold mineralization is hosted in milky to pinkish quartz veins, which are consistent with foliation, at a varying thickness from 10 to 30 cm and embedded in the quartzite packages. Green muscovite, siderite and biotite are found bordering these veins.

The metapelites comprise schists of distinct compositions. Generally, they are muscovite schists with varying quantities of quartz, biotite and chlorite (Fig. 9C). In the microscopic analysis, the rock shows a lepidoblastic texture and the following modal composition: muscovite (20–70%), quartz (15–40%), chlorite (5–35%) and biotite (5–40%). The accessory minerals are tourmaline, magnetite and rutile. The petrographic thin sections show carbonate, epidote and amphibole, which were used to classify some samples as metamarls. In certain outcrops, these rocks are very rich in quartz, possibly representing sheared and/or hydrothermal quartzites.

Thin lenses of carbonaceous schist 10 to 30 cm thick occur interspersed in metarhythmite outcrops characterized by the alternation of metapelite and quartzite packages (Fig. 9D).

A dolomitic marble lens with thicknesses ranging from 10 to 70 m occurs interspersed in the feldspathic quartzite packages or at its contact with pure quartzite. The lens appears very friable in the cores, which may explain why it was not observed in the outcrops during fieldwork.

The main foliation (S_n) in the study area has an average attitude of N30ºW/30ºSW, which is consistent with the attitude of the greenstone belt syncline. The mineralized quartz veins are aligned NW-SE, sub-parallel to the main foliation. However, the mineralization is controlled by intersection

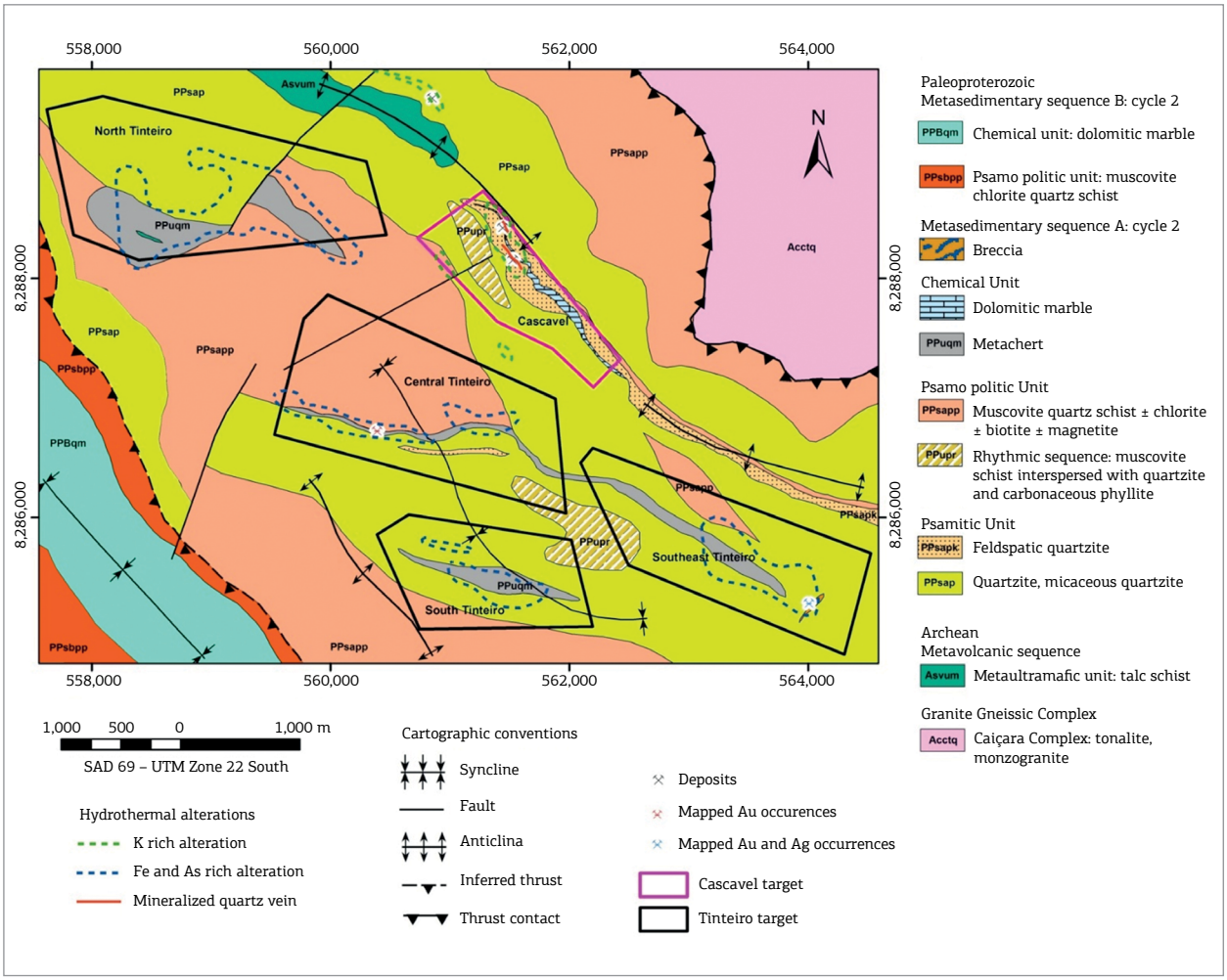

Figure 8. Geologic map of the study area at the 1:10,000 scale covering the Cascavel and Tinteiro target sites; the map was produced by integrating the geologic map created by Toledo *et al.* (2014) at the 1:25,000 scale, the geologic map from *Orinoco do Brasil Mineração Ltda.* and data obtained in this study. Boundaries of the hydrothermal alteration halos are also indicated.

lineations that have an average attitude of S80ºW/20º and formed by an intersection of two foliations (S_n and S_{n+1}) that form the shear zone (S-C foliation). In the Cascavel prospect, an intersection of regional structures is observed (NE-SW intersected with NW-SE and NE-SW crossing E-W) as interpreted from the aeromagnetic grids (Fig. 7).

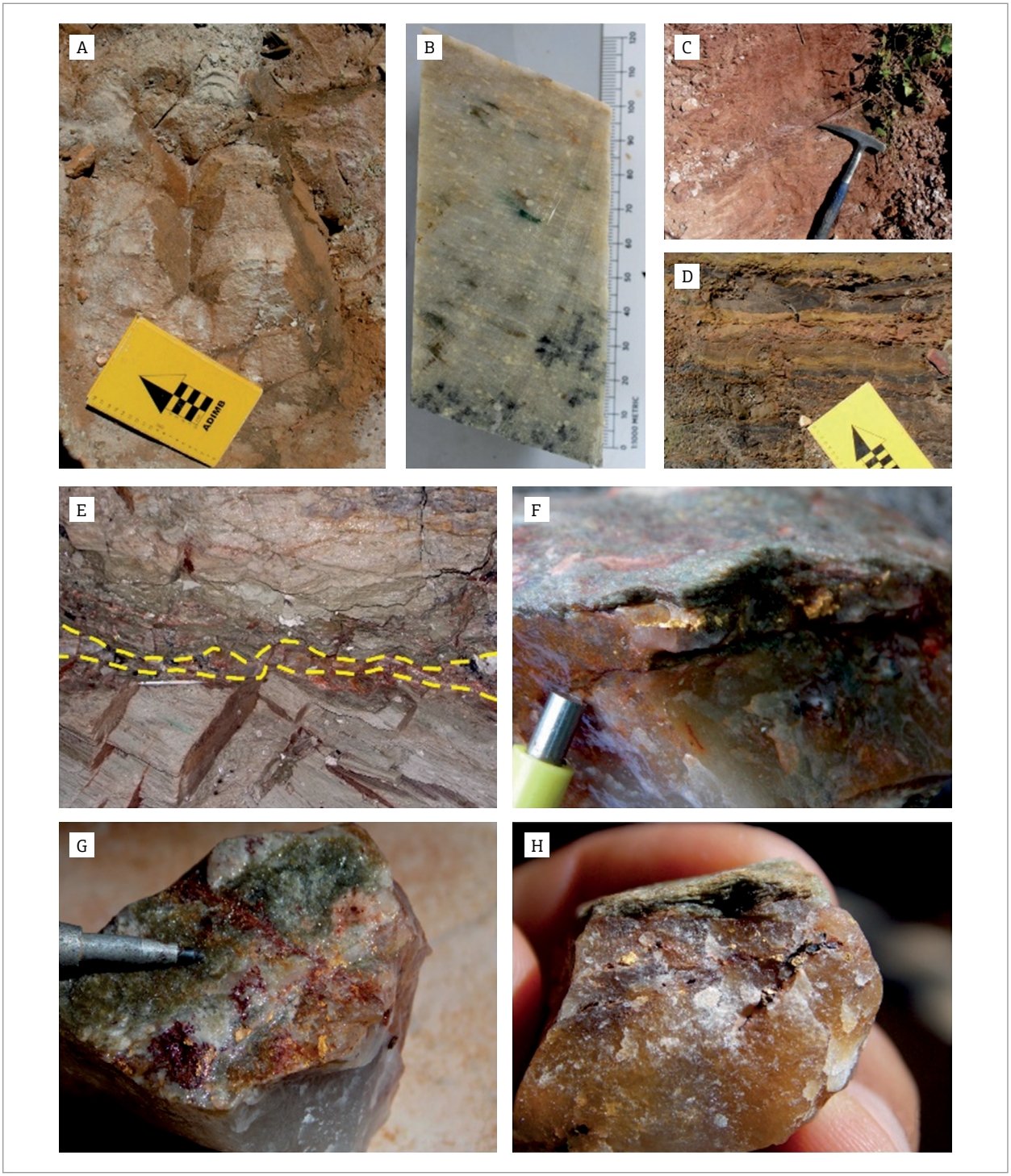

Figure 9. Main rocks found in Cascavel: (A) quartzite; (B) feldspathic quartzite; (C) weathered metapelite; (D) intercalated carbonaceous schists in metarhythmite packages. Photos of the Cascavel site gallery: (E) fine pinkish quartz vein (marked in yellow) from 10 to 50 cm thick and hosted in quartzite with green muscovite; (F), (G) and (H) spots of free gold in the quartz vein or at the contact of the vein with the host rock. Photos e, f, g and h: Orinoco do Brasil Mineração Ltda.

Hydrothermal Alteration Zones

Rock samples randomly collected along this target site were analyzed using ICP-MS. In the gallery of the Cascavel prospect, 18 anomalous samples were obtained, and they had Au concentrations varying from 11.9 to 135.5 ppm (Tab. 1). The Cascavel gallery is located in the northeast sector of the Cascavel site over a high potassium anomaly indicated in the gamma spectrometric maps, and the Cuca gallery is located to the north. The anomalous samples for gold are related to a milky to pinkish quartz vein that sometimes has visible spots of free gold (Fig. 9F-9H). The host rock of the vein is a feldspathic quartzite with green muscovite and siderite (Fig. 9E).

At this site, 44 borehole cores were obtained, and 31 of them intercepted anomalous gold levels. In addition to gold, several boreholes showed anomalous results for Ag, Pb, W, Zn and Cu in friable dolomitic marble layers that were not associated with the gold-quartz vein.

The CDP-04 and CDP-09 boreholes have been described and sampled. CDP-04 intercepted 193.69 g/t Au across 0.66 m (from 152.10 to 152.76 m depth). Other depths with anomalous gold concentrations were observed along the borehole (from 113 to 114 m, 158.1 to 160 m, 233 to 233.66 m), and anomalous concentrations of Ag, Zn, Pb and W were also observed, such as at 186.41 to 193.8 m and from 217.47 to 221.79 m (Fig. 10A). The borehole CDP-09 crossed several depths with anomalous gold concentrations (from 95 to 97 m, and from 221 to 224 m) and also had sequences with anomalous concentrations of Ag, Zn and W (from 135 to 139.13 m, and from 295 to 296 m) (Fig. 10B). In both boreholes, the gold mineralized layers are associated with quartzite packages or near their contact with metapelites. The other anomalous elements (Ag, Zn, Pb and W) are associated with the friable dolomitic marble layers.

Table 1. Rock samples from the Cascavel site gallery.

Sample	Au content (ppm)	Description
1694	59.6	Quartz veins with visible gold
1695	52.2	Quartz veins and quartzite (wall rock)
1696	42.2	Quartz veins with visible gold
1697	31.3	Quartz veins with visible gold
1698	61.8	Quartz veins and quartzite (wall rock)
1699	92.1	Quartz veins and quartzite (wall rock)
1701	39.4	Quartz veins and quartzite (wall rock)
1702	121.5	Quartz veins and quartzite (wall rock)
1703	112.5	Quartz veins with visible gold
1704	30.8	Quartz veins with visible gold
1705	35.5	Quartz veins and quartzite (wall rock)
1706	135.5	Quartz veins and quartzite (wall rock)
1707	67.7	Quartz veins and quartzite (wall rock)
1709	79.3	Quartz veins with visible gold
1710	11.9	Quartz veins with visible gold
1711	22.1	Quartz veins with visible gold
1712	12.25	Quartz veins with visible gold
1713	21.7	Quartz veins with visible gold

The hydrothermal alteration halos were classified into three zones: mineralized zone, proximal zone and distal zone, with the latter subdivided into distal 1 and distal 2.

The mineralized zone contains the inner halo of the hydrothermal alteration, which has thicknesses varying from a few centimeters to approximately 4 m, which was also observed in borehole CDP-04 (151.00 to 154.41 m). The mineral assemblage is composed of quartz, green muscovite, siderite and free gold, indicating a silicification and potassic alteration. This zone is hosted mainly within feldspathic quartzites or in metapelite layers near the contact with quartzite. The muscovite found in this area is formed from biotite.

The proximal zone is characterized by green muscovite and sometimes magnetite/hematite, and it shows potassic alteration. The thickness is highly variable and uncertain. However, field data suggest that it may be approximately 150 m. This zone is primarily hosted in quartzite packages, but also occurs in metapelites.

The distal zone is hosted mainly within metapelites, forming biotite-chlorite schists. The distal zone 1 is formed by altered biotite and calcite and can be considered an alteration step prior to distal zone 2 because it appears incomplete compared with the latter. This alteration can be observed in the chemical analysis of the biotites in the thin section 4_236.6 obtained from borehole CDP-04 (Fig. 10A), which belongs to distal zone 1 and appears to be unstable and has lost potassium and iron to the point of almost forming chlorite. In distal zone 2, chlorite is already almost completely formed.

Distal zone 2 is characterized by the assemblage chlorite, calcite and epidote, indicating a typical calcic alteration, which is observed at depths of 84 and 117.5 m in the boreholes CDP-04 and CDP-09, respectively (Fig. 10).

Geochemistry

In the Cascavel prospect, high concentrations of Zn, Cu, Pb, Ag and W, as well as the pathfinder elements (*e.g.*, Ni, Co, Cr), were found in some borehole layers.

Figure 11 shows the concentrations of Au, Ag, Cu, Zn, Ni, Co, Cr, Pb and W at the different borehole depths and

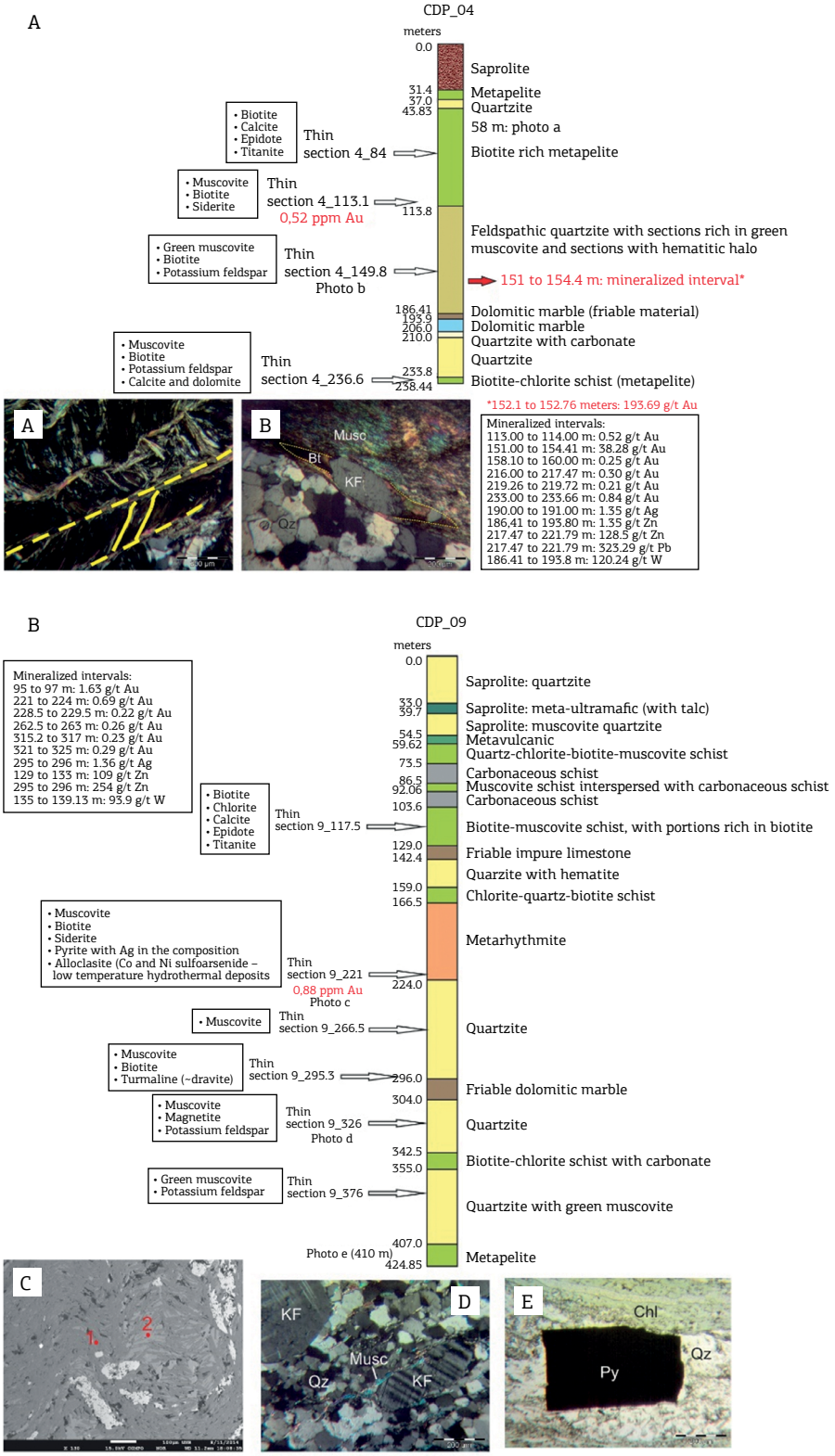

Bt: biotite; KF: potassium feldspar; Musc: muscovite; Qz: quartz; Py: pyrite; Chl: chlorite.

Figure 10. (A) Description of the borehole CDP-04 showing mineralized layers. Photomicrography: a) S-C foliation marked by muscovite in quartz-muscovite schist; and b) deformed potassium feldspar, showing pressure shadows filled with biotite. The muscovite is older than the biotite. (B) Description of the borehole CDP-09 showing mineralized layers. Photomicrography: c) hydrothermal muscovite (1) formed from biotite (2); d) feldspathic quartzite with muscovite; and e) late euhedral pyrite.

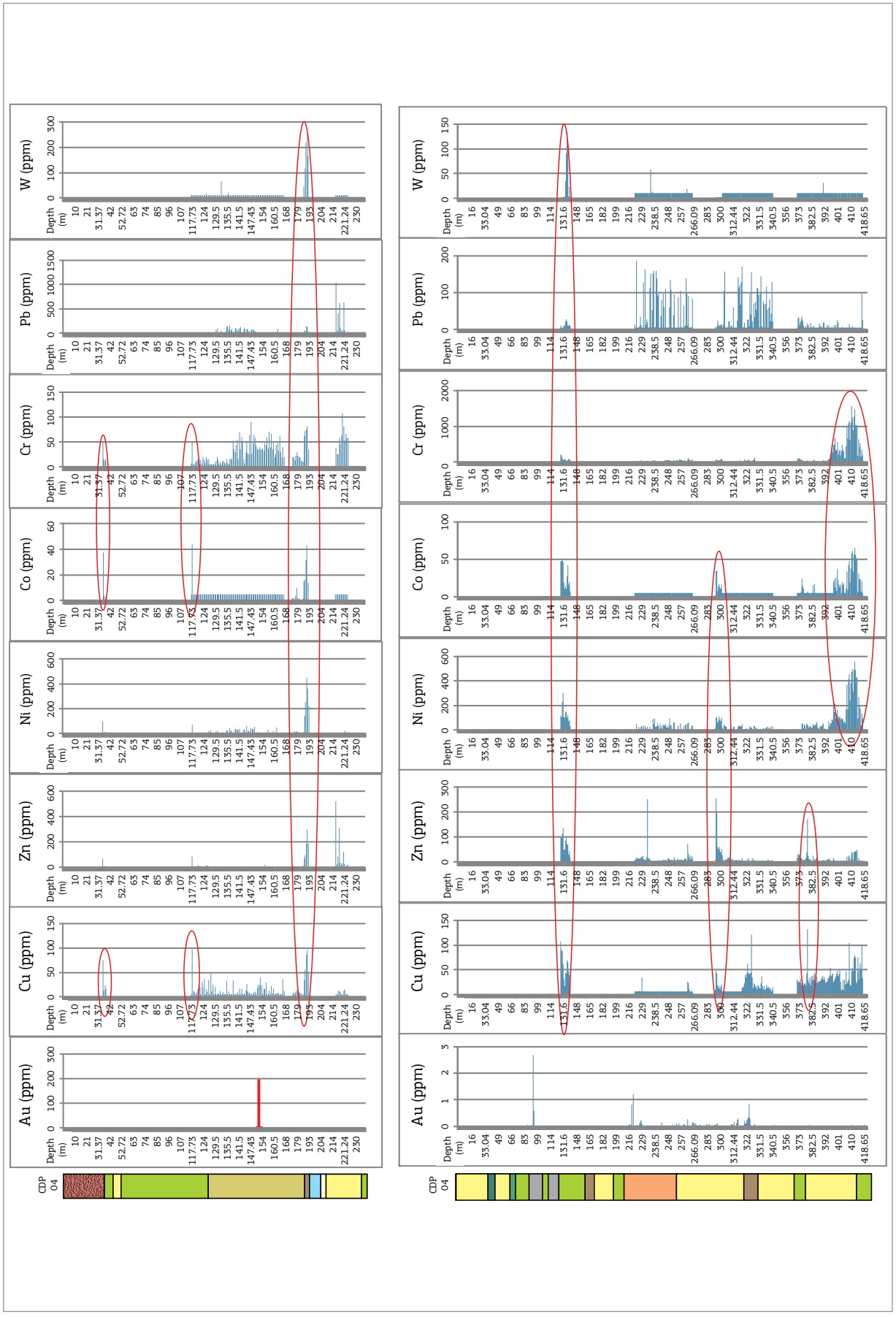

Figure 11. Distribution of the elements Au, Cu, Zn, Ni, Co, Cr, Pb and W (in ppm) along the boreholes CDP-04 and CDP-09, and possible correlations (red circles).

indicates that a correlation occurred among Cu-Zn-Ni-Co-Cr-W, which are primarily associated with the friable dolomitic marble layer. For borehole CDP-04, there were correlations among Cu-Co-Cr, and in CDP-09, the correlations include Cu-Zn-Ni-Co, Cu-Zn and Ni-Co-Cr. Gold in both boreholes did not show a correlation with other elements.

Mineral Exploration Vectors

By processing and interpreting the geophysical, geochemical and geological data available, the main exploration vectors were identified and subsequently used in the production of the final prospectivity map. These vectors are summarized in Table 2 and discussed later in the article.

Tinteiro Target

Lithological and Structural Controls

The Tinteiro target site is located west of Cascavel in the central greenstone region. The site is divided into four subsites: north, central, southeast and south Tinteiro (Fig. 8). The main lithotypes of Tinteiro are quartzite, feldspathic quartzite, metapelite, metachert and talc schist, which belong to the metasedimentary sequence A (Fig. 8). Gold, copper, silver and iron mineralizations often occur associated with the metachert and take the form of hematite breccias, manganiferous breccias or gossan.

The quartzite (Fig. 12A) is fine to medium grained and occurs as massive outcrops that are usually found at the bottom of streams in a wide range of colors, including white, yellowish, pinkish and grayish, and it has a granoblastic texture. The modal composition comprises quartz (60–85%) and muscovite (5–30%) as the major minerals, and magnetite, tourmaline and sulphides the accessory minerals. Alterations rich in iron oxides are common. A feldspathic quartzite lens intruded in the quartzite occurs in the south section of Central Tinteiro, and it is similar to the feldspathic quartzite lens found in Cascavel.

The metapelites have a lepidoblastic texture, and they form schists with variable compositions and concentrations of muscovite (20–60%), chlorite (5–20%) and quartz (10–30%) (Figs. 12B and 12C). The metapelites are usually thinly layered and of greenish color or reddish when weathered. Pyrite and magnetite crystals occur locally. In South Tinteiro, fine-grained greenish chloritoid lenses occur within the metapelite.

The metacherts are rocks formed primarily by quartz (60–90%) and muscovite (5–20%), and they have a gray color and fine banding (Figs. 12D and 12E). These rocks generally form lenses with thicknesses varying from a few centimeters to approximately 500 m, and they are hosted at the contact between the quartzite and the metapelite or within the quartzite packages.

In the north Tinteiro, talc schist lenses characterized by a silky appearance and the presence of cubic pyrite crystals occur embedded in the metachert.

Lineaments extracted from the first vertical derivative (Dz) (Fig. 7) occur at the target site and are aligned E-W and NW-SE. The main foliation at this site has an average attitude of N28°W/27°SW, and the average attitude of the stretching lineation is N79°W/18°, characterized by minerals stretched and axis of boudins. The northeast sector of north Tinteiro is intersected by a sinistral fault aligned N50°E and parallel to the Faina Fault.

The structural controls of mineralization are not fully clear in Tinteiro because, in certain locations, mineralization is intersected by ductile and brittle structural features, such as shear zones, fractures and faults aligned NE-SW, NW-SE and E-W, whereas in other locations mineralization occurs at the intersection of these structures (NE-SW with E-W and NE-SW with NW-SE).

Hydrothermal Alteration Zones

The hydrothermal alteration zones found in all Tinteiro sub-sites are similar. Metapelite, quartzite and metachert outcrops (especially) usually show ferric alterations formed by massive goethite and/or hematite associated

Table 2. Main mineral exploration vectors identified in the Cascavel target site.

Exploration Vectors: Cascavel Target		
Geophysical Vectors	**Geochemical Vectors**	**Geological Vectors**
Low amplitude	Au anomalous	Intersection of NW-SE, E-W and NE-SW structures
Low magnetic gradient	Some anomalies Cu	
High K values	K rich alteration	Mineralization next to lithological contacts
		Mineralization in quartz veins

with intense silicification. The ferric alteration produces a banded appearance of the mineralization host rocks and often leads to the incorrect classification of a number of units in the Tinteiro site as banded iron formations (Fig. 13A). Hydrothermal green muscovite is commonly found associated with or close to these alterations hosted in quartzites, metacherts and metapelites, especially in the borehole cores.

Mineralization occurs in association with hematite breccias (Figs. 13A–13C), manganiferous breccias (Fig. 13D) and gossan. The breccias are characterized by angular fragments of metachert cemented by metallic material of gray

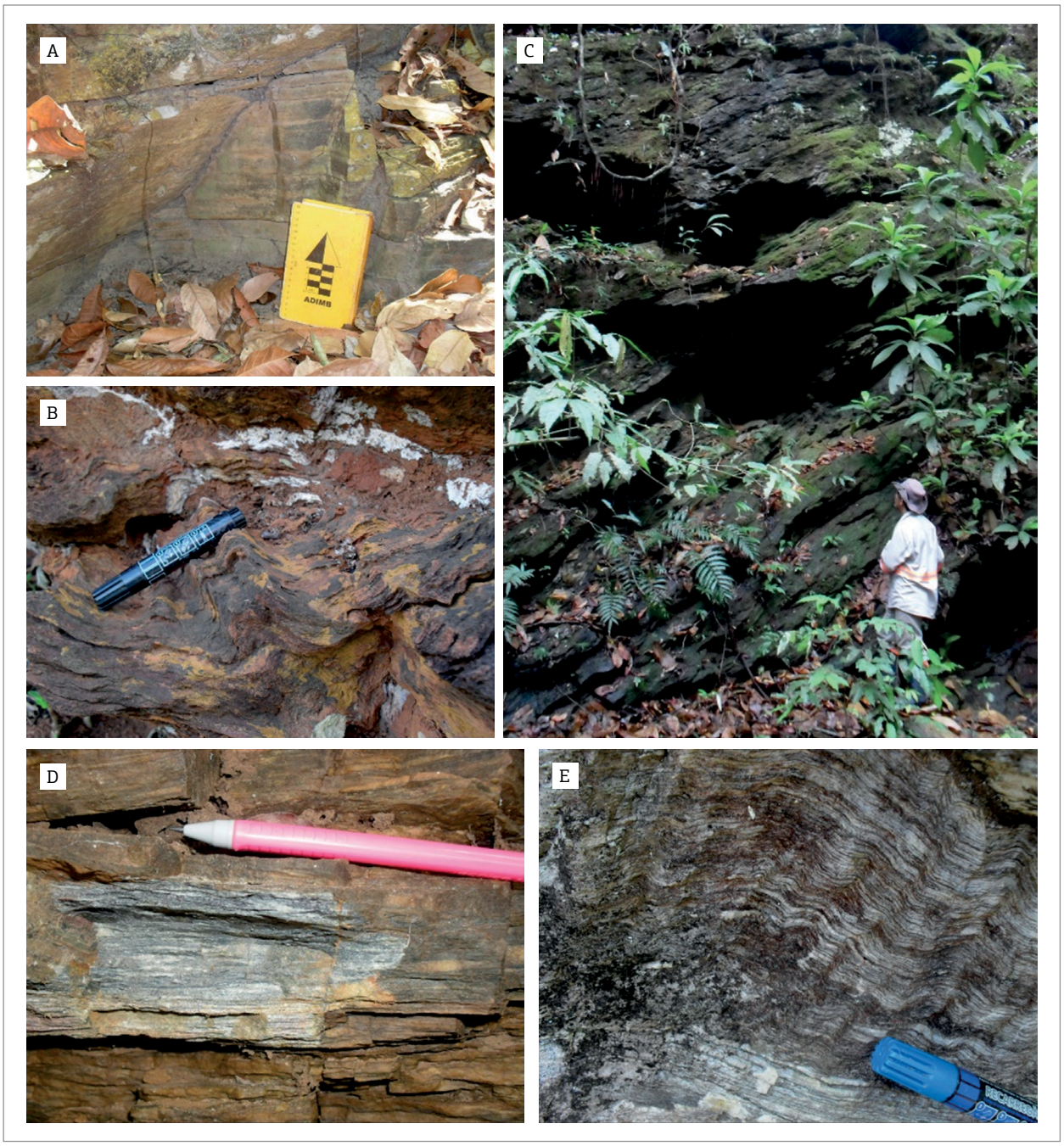

Figure 12. Photos of the rocks found in Tinteiro prospect: (A) massive and gray quartzite with muscovite; (B) weathered and folded quartz-muscovite schist; (C) greenish quartz-chlorite-muscovite schist; (D) massive metachert is composed mainly by quartz; (E) finely laminated metachert showing bands rich in quartz alternated with bands rich in muscovite and biotite.

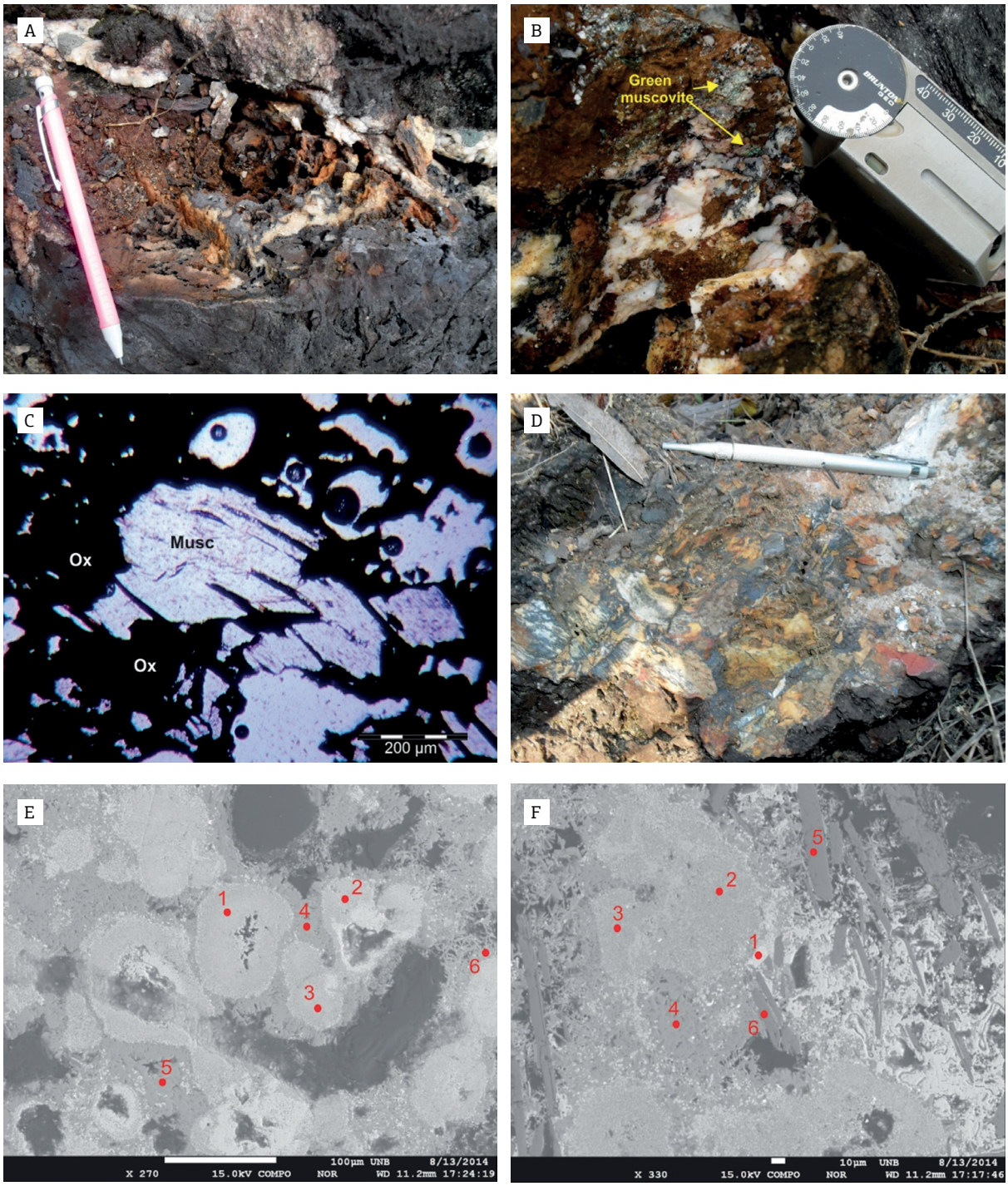

Musc: muscovite; Ox: oxides, such as goethite and hematite.

Figure 13. (A) Hydrothermal alteration of the Tinteiro site, which shows solid portions of goethite/hematite in metachert, consisting of hematite breccia; (B) hematite breccia is highly weathered and contains green muscovite; (C) photomicrography of the metallic gray cement of the hematite breccia; (D) detail of the breccia formed by irregular fragments of metachert cemented by metallic bluish gray material; (E) and (F) backscatter images of the manganiferous breccia cement showing that (E) 1, 2 and 3 are hollandite (lighter) and 4, 5 and 6 are lithiophorite (darker); (F) 1 is hollandite, 2, 3 and 4 are lithiophorite, and 5 and 6 are muscovite.

coloration if it is rich in hematite or bluish when rich in manganese. The gossan occurs as brown weathered layers embedded in quartzite or metachert.

The hydrothermal alteration zones were classified into two zones: a mineralized zone and the proximal alteration zone.

The proximal alteration zone is composed of ankerite, magnesium siderite, chlorite and muscovite. The muscovite is richer in magnesium in the proximal zone than in the mineralized zone.

The mineralized zone is characterized by the presence of arsenopyrite, hematite, muscovite and free gold when associated with hematite breccias or gossan. The arsenopyrite occurs completely altered and forms goethite. The goethite chemical analyses show high concentrations of arsenic, revealing the origin of this mineral. A number of arsenopyrite crystals contain gold and/or silver in the inner structure.

Ilmenite and rutile crystals are common in this zone and interpreted as resulting from biotite alterations. A number of samples present monazite crystals.

When associated with manganiferous breccias, the mineralized zone is characterized by the presence of manganese oxides and muscovite. Backscatter images of an oxide sample extracted from the metallic blue cement are shown in Figures 13E and 13F. The image shows mineral zonation formed from lighter and darker zones as well as muscovite crystals. The chemical composition of these oxides indicate that they can be classified as hollandite ($Ba(Mn^{+4},Mn^{+3})_8O_{16}$), which forms the lighter zone, and lithiophorite ($(Al,Li)Mn^{+4}O_2(OH)_2$), which forms the darker zone (Figs. 13E and 13F).

Hollandite is a manganese oxide rich in barium and found as a secondary mineral in oxidized zones of manganese deposits, as a primary mineral in contact metamorphism, in deposits showing hydrothermal veins (Post 1999).

Lithiophorite is a manganese oxide with lithium that is often found in weathered zones of manganese deposits or in low-temperature hydrothermal veins (Post 1999). The eletron microprobe analysis does not measure concentrations of lithium; however, the ICP-MS analyses of the breccia samples show anomalous concentrations of lithium at 178.2, 230 and 560 ppm, which verified its identification.

Chemical analyses of the breccia show anomalous concentrations of silver at 245 and 4,234 ppm, although they did not show positive results for gold. The electron microprobe analysis reveals the presence of Ag and Au as minor components of the hollandite and the lithiophorite. The concentration of silver varies from 0 to 450 ppm in some of these minerals and did not appear to be correlated with any of the other elements. The concentration of gold varies from 0 to 1,510 ppm, which was higher than the silver concentrations. The samples showing higher concentrations of gold are correlated with higher concentrations of Ba, *i.e.*, with hollandite. Although high concentrations of Au appeared to be associated with hollandite, not every hollandite included Au.

The electron microprobe analyses reported considerable amounts of Ni, Cu, Co and Zn in the lithiophorite structure. This result corroborates the chemical analyses conducted by Post (1999), who indicated that Li, which is usually found at concentrations of approximately 0.2 to 3% in lithiophorites, is commonly substituted by the transition metals Ni, Cu, Co and Zn.

This breccia was intercepted by the borehole TIN-1A at depths of 1.0 and 5.74 m. The chemical analyses at this depth range revealed a strong correlation between Li, Cu, Co, Ni, Mn and Zn found in lithiophorite minerals (Fig. 14). The electron microprobe analyses of the samples extracted from this layer show high concentrations of Ag, Ba, Pb and V associated with hollandite and lithiophorite.

Geochemistry

The geochemical studies of the Tinteiro site reveal high polymetallic potential, which indicates an IOCG deposit (Swanepoel 2014). Many of the chemical elements, including Ag, Cu, Fe, Co, Ni, Zn, Mn, Li, Ba and V, show positive responses at all four sub-sites. These results have been obtained from the geochemical maps generated according to the rock and soil samples.

The North Tinteiro site is rich in iron at concentrations reaching up to 50%, mainly in the western sector. Iron shows a weak correlation with zinc and copper and is inversely correlated with silver and tungsten, which in turn are mutually correlated. Gold occurs in concentrations of up to 10.25 ppm and is always associated with samples rich in iron and, in certain samples, copper. The strongest correlations found at the site are with barium, nickel and chromium, with the latter occurring in concentrations of up to 2,045 ppm, the highest across all Tinteiro sub-sites.

Central Tinteiro shows the highest concentrations of all Tinteiro sub-sites for elements, such as Au (23.9 ppm), Co (10,000 ppm), Cu (3,995 ppm), Mn (168,200 ppm), Ni (5,600 ppm), Pb (216 ppm) and Zn (2,580 ppm). These elements are not spatially correlated because they occur dispersed across the site.

Southeast Tinteiro is characterized by the presence of manganiferous breccia in the southeastern sector and shows strong Ag, Ba, Co, Cu, Li, Mn, Ni, V and Zn anomalies. Most noticeable are the high concentrations of silver and lithium at up to 4,234 ppm and 560 ppm, respectively.

South Tinteiro shows anomalous concentrations of Co, Cu, Li, Mn and V, and the rocks at this target site are composed of up to 59.3% iron and vanadium at concentrations reaching 5,930 ppm, which is the highest value across all Tinteiro sub-sites.

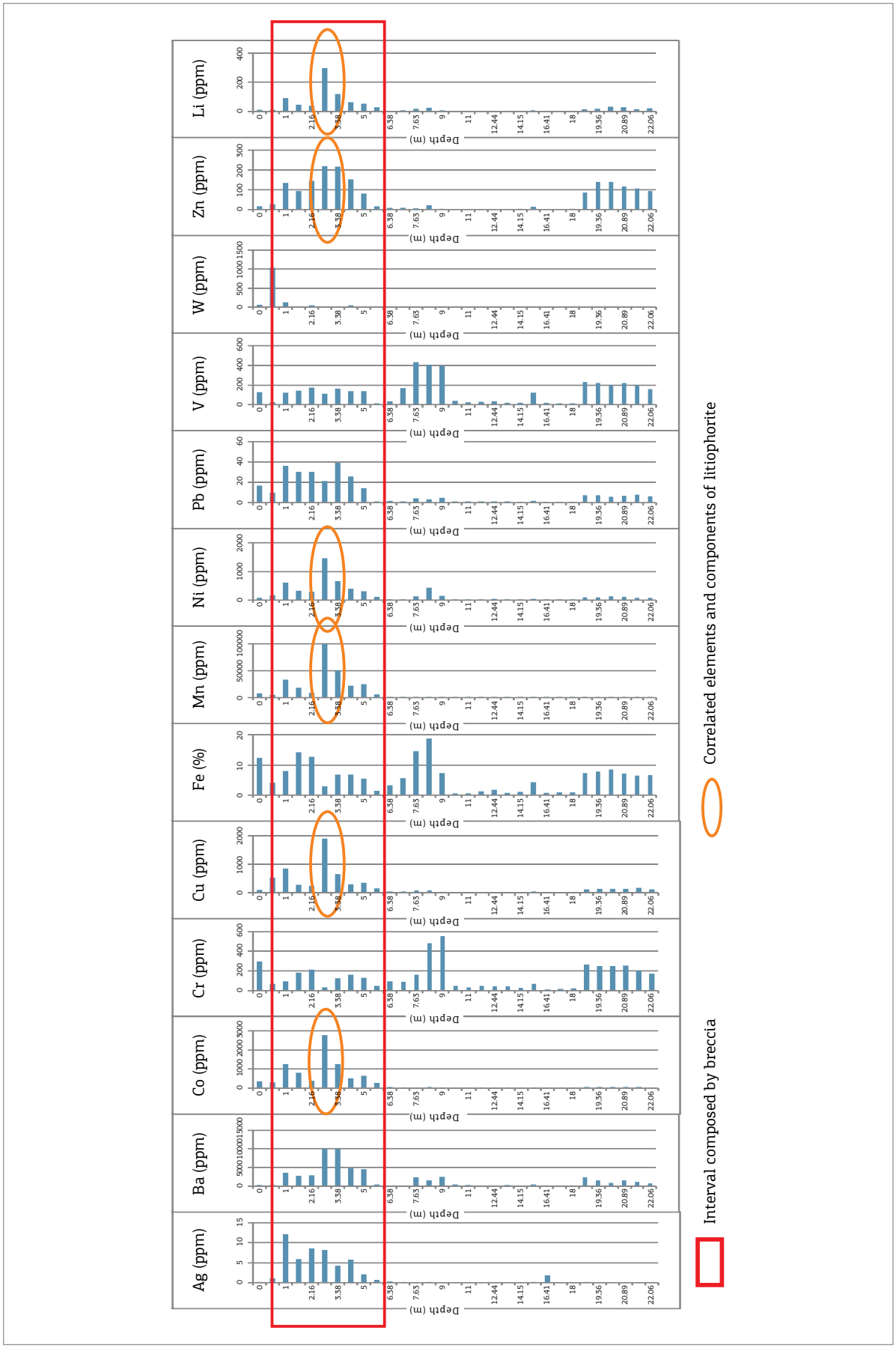

Figure 14. Chemical analyses of the borehole TIN-1A, highlighting the layer intercepting the manganiferous breccia and showing anomalous concentrations of Ag, Ba, Pb and V in addition to Co, Cu, Mn, Ni, Zn and Li, which occur in the lithiophorite structure.

Mineral Exploration Vectors

The main exploration vectors covering the Tinteiro site are described in Table 3.

Data Integration in Prospectivity Maps: Selecting New Target Sites

Fuzzy logic has been shown to be an efficient tool in the search for new prospecting targets; therefore, it has been widely used in mineral study projects of various types and scales (Nykänen *et al.* 2008). This technique is an approach based on expert knowledge and converts semantic descriptions into numerical spatial models that predict the location of the object of interest (Raines *et al.* 2010). The application of this method in the study area aims to show zones with similar geophysical, geochemical and geological signatures, thus indicating potential gold or polymetallic mineralization hosts. In recent decades, the application of this methodology has provided excellent results in areas where limited information is available, and it has provided high-level prospecting scenarios in established mining areas (Nykänen 2008, Silva *et al.* 2012).

The fuzzy methodology was applied to create the prospectivity maps for Cascavel and Tinteiro sites. The models used in this study have been suggested by Nykänen (2008) for applications in orogenic gold and IOCG deposits. The geologic input data included lithology and structures controlling gold mineralization at each target site. The geophysical images used included ASA, Dz, F factor and eU (ppm) because they represent important prospecting vectors in the region. The geochemistry model included concentrations of gold and silver in addition to Fe, Cu, Co and As, which is related to sulphidation and oxidation, and K in potassic alteration zones.

Fuzzy logic can use values between 0 and 1 (Raines *et al.* 2010), in which 0 represents "no membership" and 1 represents "full membership" data (*i.e.*, 100% chance of occurring). Therefore, all of the data used in the models were reclassified according to this scale using fuzzy membership functions, including fuzzy categorical, fuzzy large and fuzzy small. The next step consists of selecting the fuzzy operator that best represents the data interactions. The following operators were used: fuzzy AND, fuzzy OR and fuzzy gamma, which is a combination of fuzzy sum and fuzzy product (An *et al.* 1991, Bonham-Carter 1994). In conditions in which $\gamma = 1$, the combination will be equal to the fuzzy sum, and in conditions where $\gamma = 0$, the combination will be equal to the fuzzy product (Nykänen *et al.* 2008).

The fuzzy categorical function was applied for the lithological and structural data. In the lithologies with greater potential for mineralization, the fuzzy values were higher (equal or close to 1), whereas the less mineralized rocks received values equal or close to 0 (Tab. 4). Therefore, the mineralized manganiferous breccia found in the southeast Tinteiro site received a value equal to 1 and, the Cascavel dolomitic marble received a value equal to 0 because this lithology is not associated with orogenic gold.

The mineralizations occurring in the target sites appear to be related to more than one type of structures, a subject requiring further investigation. Considering this, the three main structures (NE-SW, NW-SE and E-W) identified in the geophysical maps and the Landsat 7 ETM+ image were used in the fuzzyfication process. A value equal to 0.9 was assigned to sites at which one of the three structure types was present and a value equal to 0.5 was assigned to sites at which the three types of structures were not observed. The influence area measured in the field differs for the three

Table 3. Main mineral exploration vectors identified in the Tinteiro target site.

Exploration Vector: Tinteiro Target		
Geophysical Vectors	**Geochemical Vectors**	**Geological vectors**
High amplitude	Au, Ag, Cu, Fe, Co, Mn, Li, Ba, Ni anomalous	Intersection of NW-SE, E-W and NE-SW structures
High magnetic gradient		
High eU values	Fe and As rich alteration	Mineralization in metachert and metapelitic
		Gossan and breccias occurrences

Table 4. Fuzzy membership values assigned to each lithology.

Cascavel Target		Tinteiro Target	
Lithology	**Fuzzy membership**	**Lithology**	**Fuzzy membership**
Feldspathic quartzite	0.8	Breccia	1.0
Metapelitic	0.4	Metachert	0.9
Quartzite	0.3	Feldspathic quartzite	0.8
Metarritmite	0.2	Metapelitic	0.4
Dolomitic marble	0.0	Quartzite	0.3
		Metarritmite	0.2
		Talc schist	0.0

types of structures (100 m for structures aligned NE-SW, 80 m for structures aligned NW-SE and 50 m for structures aligned E-W). The fuzzy operator AND was applied to integrate the three structures and identify their intersection.

The other geophysical and geochemical data were interpreted, reclassified (fuzzy membership) and integrated (fuzzy operators) separately for each site. Although the Cascavel and Tinteiro sites are spatially close, they have different characteristics, with the gold mineralization in Cascavel hosted in an orogenic deposit and the polymetallic mineralization in Tinteiro of the IOCG type.

The Tinteiro site was subdivided into the sub-sites north, central, southeast and south, with each covered in specific models. Geochemical differences are the main differences between each sub-site, with silver anomalies only found in the southeast and south sub-sites and cobalt found in the central and southeast sub-sites. Iron, Au, Cu and As were used in all models.

Cascavel Target

The gold mineralization of the Cascavel deposit is found in an area of low magnetic amplitude with high concentrations of radioelement K (Tab. 2). The aeromagnetic data are corroborated by the measurements indicating low magnetic susceptibility. Based on these results, ASA and Dz were used in the fuzzy small function and the F factor was used in the fuzzy large function. Subsequently, the fuzzy operator AND was used to identify the intersection between Dz and the F factor, which produced conservative results (Fig. 15A).

In the geochemical model, fuzzy large was used for Au, K (because of the potassic alteration characteristic of the mineralized zone), Fe, As and Cu. Fuzzy OR was used for Fe and As to assess each element individually, and then fuzzy AND was used for Cu and the results from the previous operation. Fuzzy gamma at $\gamma = 0.9$ was applied to integrate the geophysical, geochemical, lithological and structural data, thus generating the prospectivity map shown in Figure 16.

The high-favorability regions are associated with feldspathic quartzite. The model shows that the Cascavel deposit is located on top of the favorable region.

Tinteiro Target

This site is characterized by the presence of gold mineralization and Ag, Fe, Co, Cu anomalies, amongst others.

The geophysical characteristics shown in Table 3 were used to apply fuzzy large to ASA and eU, and the fuzzy operator AND was applied to both, thus identifying the intersections. Fuzzy small was applied to Dz.

For all of the sub-sites, fuzzy large was applied for Fe, Cu and As (associated with sulphitation) and followed by fuzzy AND, and these functions were integrated in the models (Figs. 15B-15E). Fuzzy large for Co was incorporated in the central Tinteiro and southeast Tinteiro models because this element shows concentrations above 10,000 ppm in these areas (Figs. 15C and 15D). Fuzzy large for Au was applied across all Tinteiro sub-sites and integrated with fuzzy large for Ag through the fuzzy operator OR in the southeast and south Tinteiro sub-sites. Figure 17 and 18 show the prospectivity maps produced for Tinteiro using fuzzy gamma with $\gamma = 0.7$.

All of the prospectivity maps show high-favorability regions for mineralization. The main lithology associated with high favorability is metachert, which is apparent in the four Tinteiro sub-sites. North Tinteiro shows two main high-favorability regions: one in the southeast sector and the other one in the southwest sector. In the latter, a refined soil grid was used, which presented positive results for gold. In this sub-site, medium-favorability regions (0.71–0.80) occur in association with metapelites. In central Tinteiro, there are seven main high-favorability regions associated with metachert and metapelite. Boreholes TIN-04 and TIN-05 were obtained from one of these regions in the southwest region of the site, with TIN-04 showing positive results for gold and silver and TIN-05 only showing positive results for silver. In southeast Tinteiro, five high favorability regions were identified, with four associated with metachert and the fifth associated with manganiferous breccia. Boreholes TIN-1, TIN-1A, TIN-2 and TIN-3 cross this breccia layer and show anomalous concentrations for many elements, including silver, copper, cobalt, manganese, barium and lithium. In south Tinteiro, five favorable regions were identified in association with metachert and with quartzite (in the northern sector). The soil samples do not present good correlations with these areas because the positive results for gold are found across the entire sub-site.

VALIDATION AND EVALUATION OF THE BEST PREDICTORS

All of the prospectivity maps generated in this study show high-favorability areas, suggesting a new direction for exploration studies at the target sites. However, the question of whether the resulting model is reliable remains to be answered.

In Cascavel, four regions showing first-order favorability are identified in the prospectivity map. The Cascavel deposit is within the largest of these regions, where 18 rock samples from the gallery show anomalous gold concentrations (between 11.9 and 135.5 ppm) and other samples

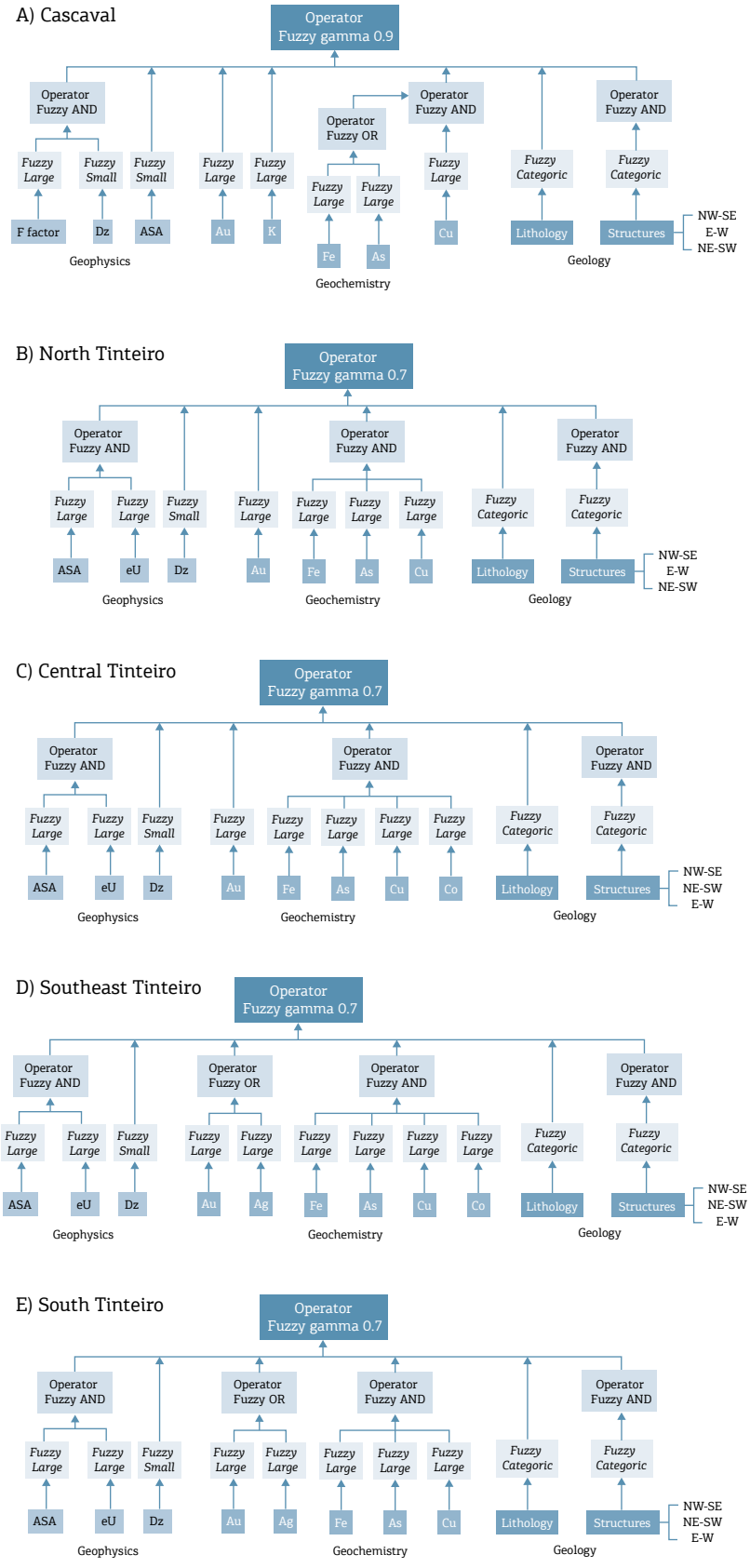

Figure 15. Flowchart representing the steps of the fuzzy logic method for: (A) Cascavel; (B) North Tinteiro; (C) Central Tinteiro; (D) Southeast Tinteiro, and (E) South Tinteiro.

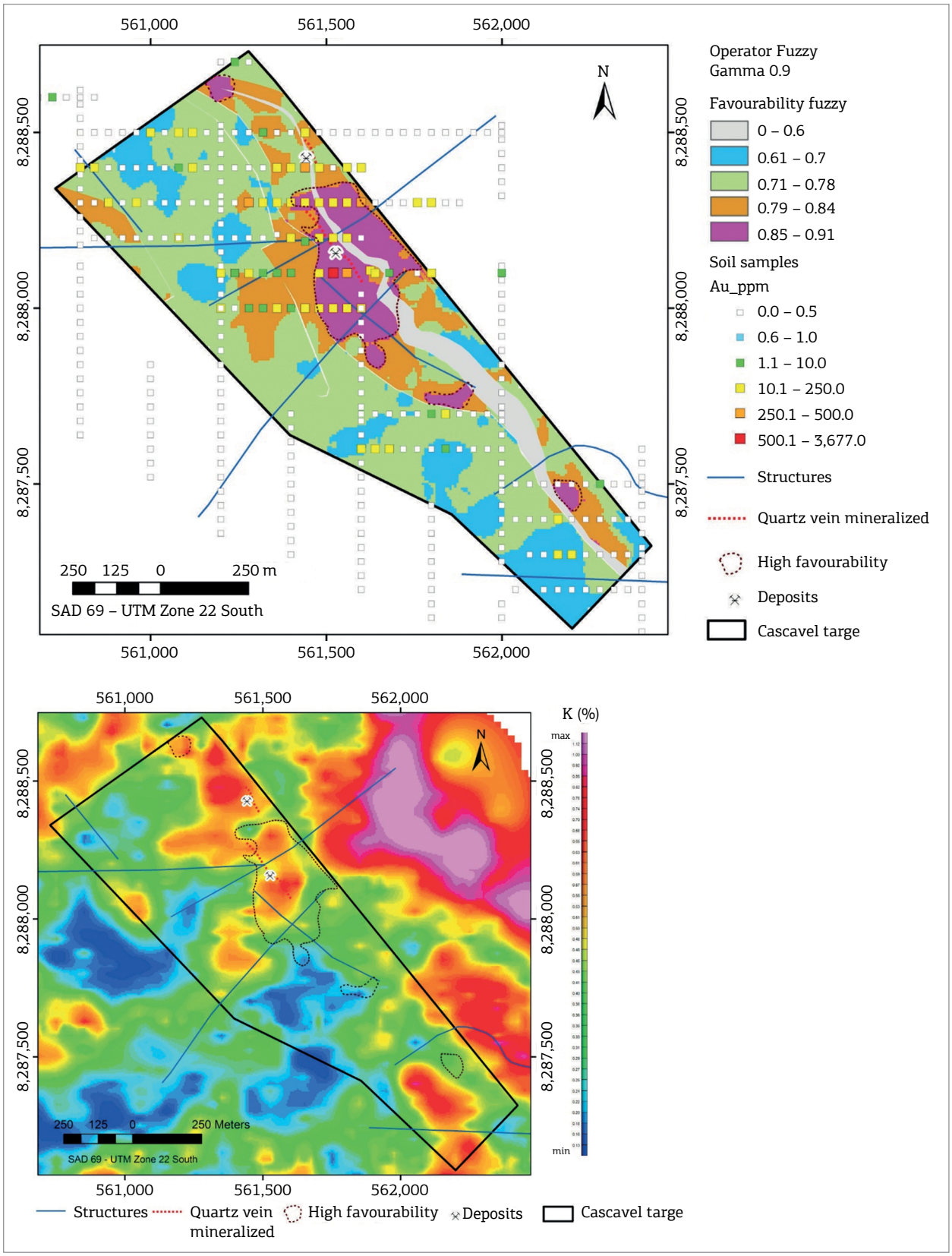

Figure 16. Prospectivity map for the Cascavel site integrated with the soil grid, mineralized quartz veins associated with the Cascavel deposit, and the main lineaments identified from aeromagnetic images. The soil grid refinement over the area showing the highest favorability indicates an anomalous concentration of gold in this region. The concentration of the radioelement K (%) indicates that the region of highest favorability is associated with high K concentration.

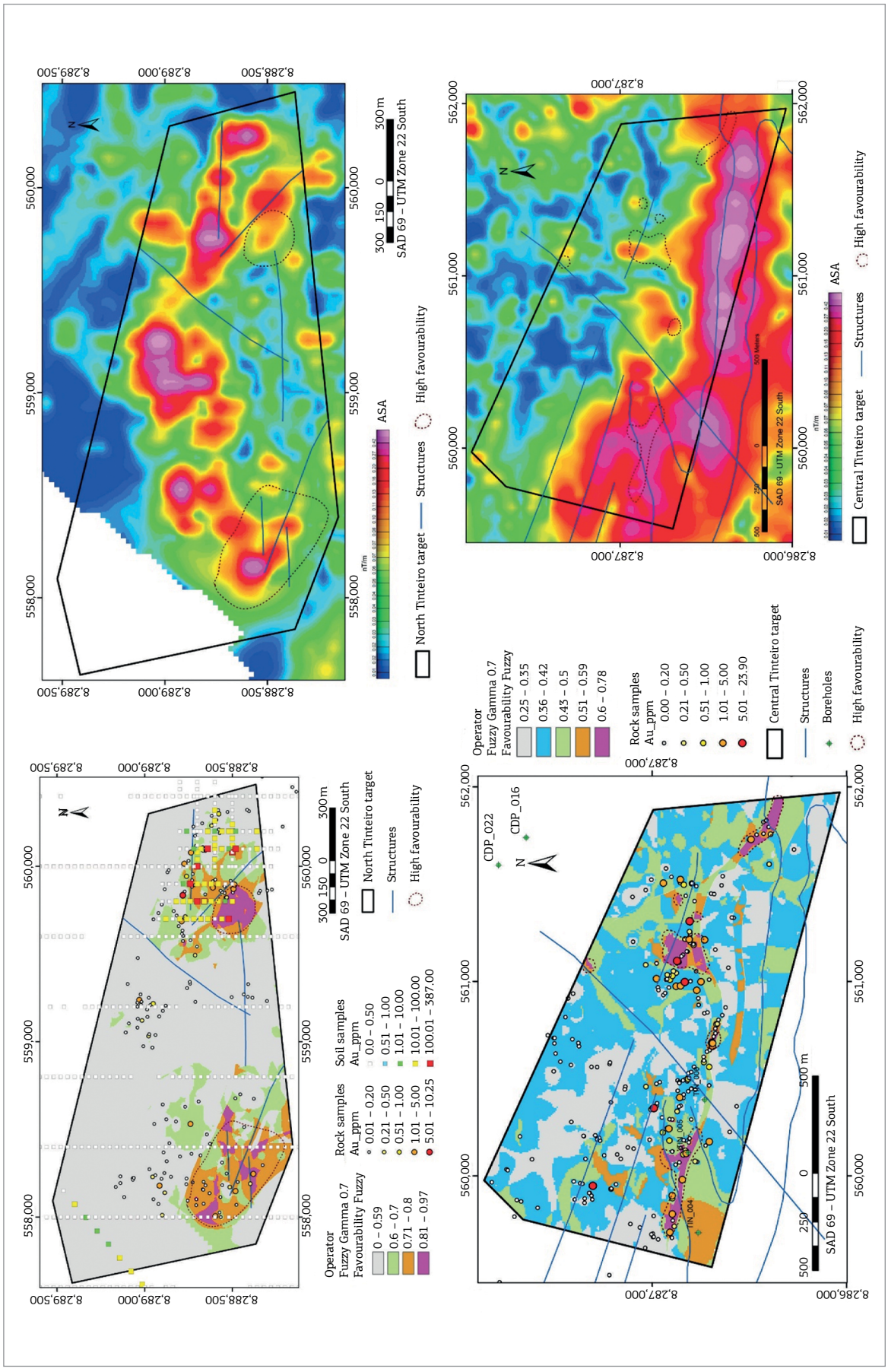

Figure 17. Prospectivity map for the Tinteiro site: (A) North Tinteiro; and (B) Central Tinteiro. The integration of the prospectivity maps with the results from the chemical analyses on the rock and soil samples and the cores validated certain high-favorability zones. These zones are intersected by lineaments and associated with high magnetic amplitudes.

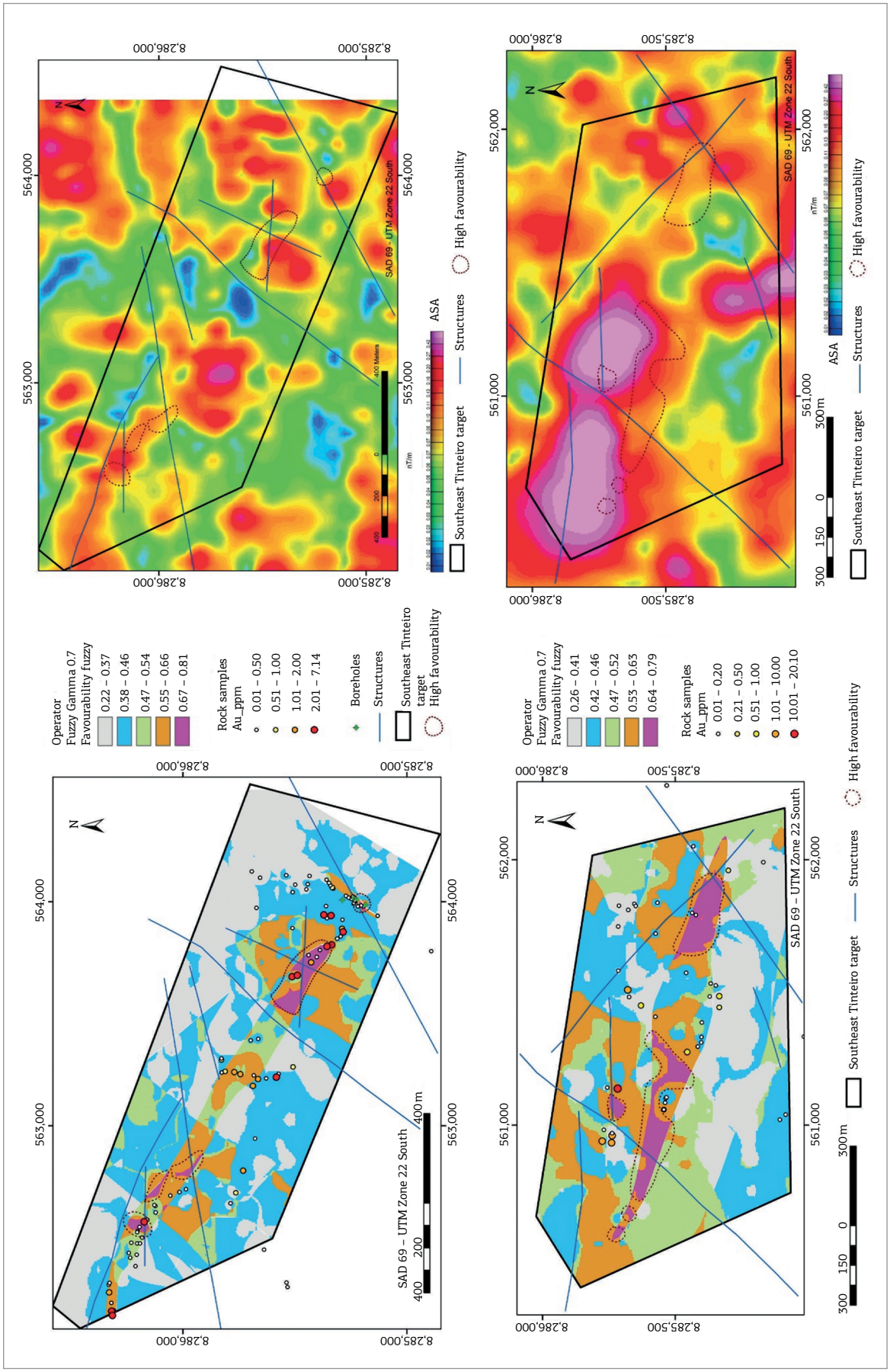

Figure 18. Prospectivity map for the Tinteiro site: (A) Southeast Tinteiro; and (B) South Tinteiro. The integration of the prospectivity maps with the results from the chemical analyses on the rock and soil samples and cores validate some high-favorability zones. These zones are intersected by lineaments and are associated with high magnetic amplitudes.

have visible gold. Within the Cascavel site, 44 cores were obtained, 27 of which reached mineralized layers in the high-favorability areas, compatible with the soil anomalous gold concentrations (Fig. 16). All of these data provide a high degree of confidence for the fuzzy logic results. The largest high-favorability region occurs at the intersection of structures (shear zones, faults, fractures, lineaments), including the intersection between NE-SW with E-W and NE-SW with NW-SE. The mineralized quartz veins of the Cascavel deposit and the Cuca mining site (north of Cascavel) are observed to be aligned NW-SE (Fig. 16), and this area coincides with the radioelement K (%) anomaly.

Tinteiro was not as thoroughly investigated as Cascavel; therefore, less data are available to validate the efficiency of the prospectivity maps. The results of the chemical rock and soil analyses occasionally coincide with regions of high favorability within all of the Tinteiro sub-sites. The results obtained from seven boreholes validated some favorable areas, three of which are in central Tinteiro and four of which are in southeast Tinteiro (Figs. 17 and 18). The ASA image reveals that all areas showing high favorability are associated with high magnetic amplitude anomalies. The high-favorability areas in all sub-sites were intersected by major lineaments aligned NE-SW, NW-SE and E-W or overlaying lineament intersections.

Therefore, the prospectivity maps reveal 19 main favorable regions in the Tinteiro site, thus suggesting a new direction in future drilling programs. In Cascavel, four new favorable sites and a number of additional locations with medium favorability (values ranging from 0.79 to 0.84) are observed, which also suggests new areas for follow up.

DISCUSSION AND CONCLUSIONS

A detailed study of all of the available data sets was undertaken to create prospectivity maps that can be used to identify the most important vectors for the resulting model. During this process, the main characteristics of the study area were identified and used to generate the final integrated map.

- Three main structural groups are identified in the study area based on the interpretation of airborne geophysical images and the RGB (453) image of the Landsat 7 ETM+ sensor. These structures are as follows: faults, shear zones and major lineaments aligned NW-SE, NE-SW and E-W. Apparently, all of the structures are related to mineralizations. However, the NE-SW lineaments are usually observed in areas where mineralization occurred in association with the intersection of structures;
- The mineralization and sedimentary deposits found at Cascavel and Tinteiro are different, with Cascavel found to be orogenic and Tinteiro found to be IOCG.

According to Groves *et al.* (1998) and Robert *et al.* (2007), orogenic deposits are characterized by their occurrence in quartz-carbonate veins, concentration along regional and secondary compressional-transpressional structures, strong lateral hydrothermal zonation proximal to distal alteration assemblages. The characteristics of the Cascavel deposit described here classify it as orogenic.

Williams *et al.* (2005) noted the following key characteristics of IOCG deposits:

1. Presence of Cu with or without Au as economic metals;
2. Hydrothermal veins, breccias and/or replacement ore styles, characteristically in specific structural sites;
3. Abundant magnetite and/or hematite;
4. Iron oxides with lower concentrations of Ti compared with the oxides occurring in igneous rocks;
5. Clear spatial association with igneous intrusions.

Comparing these characteristics with those ones observed in Tinteiro, it is possible to classify the deposits as IOCG, although the association of mineralization and igneous intrusions has not been clearly identified in this study:

- The hydrothermal alteration halo in Cascavel is characterized according to its presentation of silicification and potassification in its most inner region. The mineralization is marked by the occurrence of free gold associated with quartz, green muscovite and siderite, thus forming a mineralized zone that is primarily hosted in feldspathic quartzites;
- The hydrothermal alteration halo in Tinteiro is characterized according to its presentation of a zone rich in arsenopyrite, which is weathered to form goethite, and muscovite, thus forming a mineralized zone when associated with hematite breccias and gossan. In manganiferous breccias, the mineralized zone is formed by hollandite, lithiophorite and muscovite. Both hollandite and lithiophorite present gold and silver in their structure. The hollandite is also a source of Ba and Mn, and the lithiophorite is a source of Li, Mn, Cu, Ni, Co and Zn. The mineralization is primarily hosted mainly in metacherts and also occurs in quartzites and metapelites;
- The boreholes in Cascavel show anomalous concentrations of Au, Ag, Cu, Zn, Ni, Co, Cr, Pb and W. However, Au is not correlated to any other element. The gold mineralization is hosted in quartz veins within feldspathic quartzites, whereas the other mineralizations are associated with dolomitic marble;

- Tinteiro indicates polymetallic potential and shows anomalous concentrations of Au, Ag, Cu, Fe, Co, Ni, Mn, Ba, Pb, Zn, Cr, Li and V that are primarily associated with manganiferous breccias;
- The prospectivity map for Cascavel identified four regions of high favorability and new medium-favorability focus with probabilities between 0.79 and 0.84;
- The prospectivity maps for Tinteiro identified 19 new high-favorability foci, thus suggesting a change in direction for subsequent sampling and coring phases.

ACKNOWLEDGMENTS

The authors would like to thank Orinoco do Brasil Mineração Ltda., especially geologists M. Carvalho, V. Rodrigues, K. Araujo and T. Andrade, for supporting the development of this project. We also acknowledge the Institute of Geosciences of University of Brasília for providing access to analytical facilities, in particular Professor Nilson F. Botelho and Ricardo Lívio S. Marques, for the acquisition of microprobe data. D. S. Campos acknowledges the Brazilian Coordination for the Improvement of Higher Education Personnel (CAPES) for providing a Master scholarship (Grant 2013/15). A. M. Silva thanks the National Council for Scientific and Technological Development (CNPq) for the research grant and the support through the "Modelagem geológico-geofísica aplicada à reconstrução da arquitetura de terrenos granito-greenstone e implicações para exploração mineral: o exemplo da porção meridional do bloco arqueano de Góias" Project (Grant 474336/2013-1).

REFERENCES

Almeida F.F.M., Hasui Y., Brito Neves B.B., Fuck R.A. 1977. Províncias Estruturais Brasileiras. *In:* SBG, Simpósio de Geologia do Nordeste, 8, Campina Grande, *Anais*, p. 363-391.

An P., Moon W.M., Rencz A. 1991. Application of fuzzy set theory to integrated mineral exploration. *Canadian Journal of Exploration Geophysics*, **27**(1):1-11.

Baêta Jr. J.D., Souza J.O., Moreton L.C. 1998. Programa Levantamentos Geológicos Básicos do Brasil – PLGB. Folha SD.22-Z-C-II – Morro Agudo de Goiás; Folha SD.22-Z-C-V, Goiás; Folha SE.22-X-A-II -Sanclerlândia. Escala 1:100.000. CPRM, Goiânia, Relatório Interno.

Beghelli Jr. L.P. 2012. *Charnockitos e ortognaisses da porção Centro-Oeste do Bloco Arqueano de Goiás: dados geoquímicos e isotópicos.* MS Dissertation No. 307, Universidade de Brasília, 77 p.

Bonham-Carter G.F. 1994. *Geographic information systems for Geoscientists: Modelling with GIS*. Oxford, Pergamon, 398 p.

Carrino T.A., Silva A.M., Botelho N.F., Silva A.A.C. 2011. Lógica FUZZY e técnica SAM para modelagem previsional do ouro no setor oeste da Província Mineral do Tapajós usando dados aerogeofísicos e de sensoriamento remoto. *Revista Brasileira de Geofísica*, **29**(3):535-554.

Danni J.C.M., Dardenne M.A., Fuck R.A. 1981. Geologia da região de Goiás (GO): O "Greenstone Belt" da Serra de Santa Rita e a Sequência Serra do Cantagalo. *In:* Simpósio de Geologia do Centro-Oeste, I, Goiânia, *SBG*, p. 265-280.

Dickson B.L. & Scott K.M. 1997. Interpretation of aerial gamma-ray surveys – adding the geochimical factores. *AGSO Journal of Australian Geology & Geophysics*, **17**(2):187-200.

Evjen H.M. 1936. The place of the vertical gradient in gravitational interpretations. *Geophysics*, **1**(1):127-136.

Gnojek I. & Prichystal A. 1985. A new zinc mineralization detected by airborne gamma-ray spectrometry in northern Moravia (Czechoslovakia). *Geoexploration*, **23**(4):491-502.

Groves D.I., Goldfarb R.J., Genre-Mariam M., Hagemann S.G., Robert F. 1998. Orogenic gold deposits: A proposed classification in the context of their crustal distribution and relationships to other gold deposit types. *Ore Geology Reviews*, **13**(1-5):7-17.

Harris J.R., Sanborn-Barrie M. 2006. Mineral potential mapping: examples from the Red Lake Greenstone Belt, Northwest Ontario. *In:* Harris J.R. (ed.) GIS for the Earth Sciences. Geological Association of Canada, *Special Publication*, **44**, p. 1-21.

Jost H., Carvalho M.J, Rodrigues V.G. Martins R. 2014. Metalogênese dos greenstone belts de Goiás. *In:* Metalogênese das Províncias Tectônicas Brasileiras, CPRM, Belo Horizonte, p. 141-168.

Jost H., Chemale Junior F., Fuck R.A., Dussin I.A. 2013. Uvá complex, the oldest orthogneisses of the Archean-Paleoproterozoic terrane of central Brazil. *Journal of South American Earth Sciences*, **47**:201-212.

Jost H. & Fortes P.T.F.O. 2001. Gold deposits and occurrences of the Crixás Goldfield, central Brazil. *Mineralium Deposita*, **36**(3-4):358-376.

Jost H., Fuck R.A., Dantas E.L., Rancan C.C., Rezende D.B., Santos E., Portela J.F., Mattos L., Chiarini M.F.N., Oliveira R.C., Silva S.E. 2005. Geologia e geocronologia do Complexo Uvá, bloco arqueano de Goiás. *Revista Brasileira de Geociências*, **35**(4):559-572.

Jost H. & Oliveira A.M. 1991. Stratigraphy of the greenstone belts, Crixás region, Goiás, Central Brazil. *Journal of South American Earth Sciences*, **4**(3):201-214.

Kuyumjian R.M. & Jost H. 2006. Low- and high-alumina komatiites of Goiás, Central Brazil. *Journal of South American Earth Sciences*, **20**(4):315-326.

Nykänen V. 2008. Spatial data analysis as a tool for mineral prospectivity mapping: Espoo, *Geological Survey of Finland*, 27 p.

Nykänen V., Groves D.I., Ojala V.J., Eilu P., Gardoll S.J. 2008. Reconnaissance-scale conceptual fuzzy-logic prospectivity modelling for iron oxide copper-gold deposits in the northern Fennoscandian Shield, *Finland. Australian Journal of Earth Sciences*, **55**(1):25-38.

Pan G. & Harris D.P. 2000. *Information Synthesis for Mineral Exploration*. New York, Oxford University Press, 461 p.

Pimentel M.M., Fuck R.A., Jost H., Ferreira Filho C.F., Araújo S.M. 2000. The basement of the Brasília Fold Belt and the Goiás Magmatic Arc. *In:* Tectonic Evolution of South America. 31st International Geological Congress Special Publication, Rio de Janeiro, p. 195-229.

Pimentel M.M., Jost H., Fuck R.A. 2004. O embasamento da Faixa Brasília e o Arco Magmático de Goiás, Cap. XXI. *In:* Geologia do Continente Sul-Americano: Evolução e Obra de Fernando Flávio Marques de Almeida, p. 355-368.

Post J.E. 1999. Manganese oxide minerals: Crystal structures and economic and environmental significance. *Proceedings of the National Academy of Sciences of the United States of America*, **96**(7):3447-3454.

Queiroz C.L., Jost H., Da Silva L.C., McNaughton N.J. 2008. U-Pb SHRIMP and Sm-Nd geochronology of granite-gneiss complexes and implications for the evolution of the Central Brazil Archean Terrain. *Journal of South American Earth Sciences*, **26**(1):100-124.

Raines G.L, Sawatzky D.L., Bonham-Carter G.F. 2010. New fuzzy logic tools in ArcGis 10: ArcUser, ESRI, 13 p.

Resende M.G., Jost H., Lima B.E.M., Teixeira A.A. 1999. Proveniência e idades modelos Sm/Nd das rochas siliciclásticas arqueanas dos Greenstone Belts de Faina e Santa Rita, Goiás. *Revista Brasileira de Geociências*, **29**(3):281-290.

Resende M.G., Jost H., Osborne G.A., Mol A.G., 1998. Stratygraphy of the Goiás and Faina greenstone belts, Central Brazil: A new proposal. *Revista Brasileira de Geociências*, **28**(1):77-94.

Robert F., Brommecker R., Bourne B.T., Dobak P.J., McEwan C.J., Rowe R.R., Zhou X. 2007. Models and Exploration Methods for Major Gold Deposit Types. *Ore Deposits and Exploration Tecnhology*, **Paper 48**:691-711.

Roest W.R., Verhoef J., Pilkington M. 1992. Magnetic interpretation using the 3-D analytic signal. *Geophysics*, **57**(1):116-125.

Sabins F.F. 1996. *Remote Sensing: Principles and Interpretation*, 3rd ed., New York, W. H. Freeman and Company,494 p.

Silva E.C., Silva A.M., Toledo C.L.B., Mol A.G., Otterman D.W., Souza S.R.C. 2012. Mineral potencial mapping for orogenic gold deposits in the Rio Maria Granite Greenstone Terrane, Southeastern Pará State, Brazil. *Economic Geology*, **107**(7):1387-1402.

Swanepoel E. 2014. Orinoco expands Cascavel Gold Project. *Orinoco do Brasil Mineração Ltda. ASX Release*. 8 p.

Toledo C.L.B., Silva A.M., Chemale Jr. F., Almeida T., Garnier J., Araujo Filho J.O., Hauser N., Botelho N.F., Jost H., Bernardi G.B., Paiva R.G., Magaldi T.T., Ferreira V.H.C.S., Magalhães H.V.B., Araujo B.V.B., Silva L.B.C., Bastos Y.M.M., Teixeira C.D., Vieira H.A., Moraes F.G.M., Neiva Jr. F.B., Mansur E.T., Soares T.M., Valle R.S.C., Silva S.P., Oliveira A.L., Martins P.L.G., Franco G.S., Lamblém H.S., Leite A.M., Fazio G., Topan J.G.O., Daldegan L.C.B., Cassemiro R.B. 2014. Projeto Faina-Goiás – Mapeamento Geológico na escala 1:25.000. Trabalho de Formatura da Universidade de Brasília.

Williams P.J., Barton M.D., Johnson D.A., Fonteboté L., Haller A., Mark G., Oliver N.H.S., Marschik R. 2005. Iron Oxide Copper-Gold Deposits: Geology, Space-Time Distribution, and Possible Modes of Origin. *Economic Geology 100th Anniversary Volume*. p. 371-405.

Available at www.sbgeo.org.br